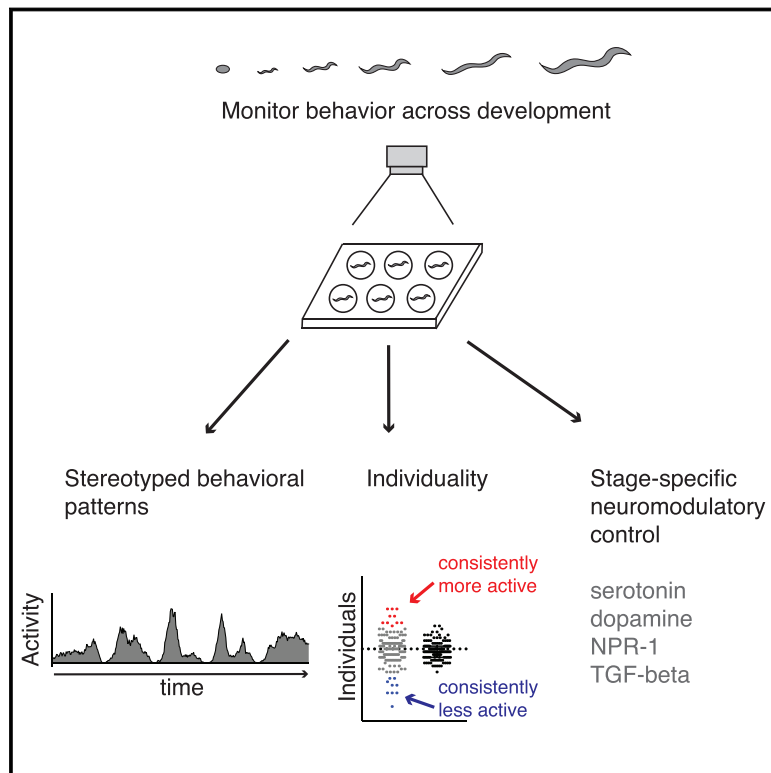


Neuromodulatory Control of Long-Term Behavioral Patterns and Individuality across Development

Graphical Abstract



Authors

Shay Stern, Christoph Kirst,
Cornelia I. Bargmann

Correspondence

cori@rockefeller.edu

In Brief

Individual nematodes exhibit consistent, non-genetic behavioral biases that are impacted by several neuromodulatory systems.

Highlights

- Long-term tracking reveals stereotyped behavioral trajectories in *C. elegans*
- Spontaneous behavior is patterned within and between developmental stages
- Some individuals have consistent, non-genetic behavioral biases
- Neuromodulation regulates stage-specific behaviors and levels of individuality

Neuromodulatory Control of Long-Term Behavioral Patterns and Individuality across Development

Shay Stern,¹ Christoph Kirst,² and Cornelia I. Bargmann^{1,3,4,*}

¹Lulu and Anthony Wang Laboratory of Neural Circuits and Behavior

²Center for Physics and Biology and Kavli Neural Systems Institute
The Rockefeller University, New York, NY 10065, USA

³Chan Zuckerberg Initiative, Palo Alto, CA 94301, USA

⁴Lead Contact

*Correspondence: cori@rockefeller.edu
<https://doi.org/10.1016/j.cell.2017.10.041>

SUMMARY

Animals generate complex patterns of behavior across development that may be shared or unique to individuals. Here, we examine the contributions of developmental programs and individual variation to behavior by monitoring single *Caenorhabditis elegans* nematodes over their complete developmental trajectories and quantifying their behavior at high spatiotemporal resolution. These measurements reveal reproducible trajectories of spontaneous foraging behaviors that are stereotyped within and between developmental stages. Dopamine, serotonin, the neuropeptide receptor NPR-1, and the TGF- β peptide DAF-7 each have stage-specific effects on behavioral trajectories, implying the existence of a modular temporal program controlled by neuromodulators. In addition, a fraction of individuals within isogenic populations raised in controlled environments have consistent, non-genetic behavioral biases that persist across development. Several neuromodulatory systems increase or decrease the degree of non-genetic individuality to shape sustained patterns of behavior across the population.

INTRODUCTION

Animal behavior is expressed on different timescales. Escape behaviors can be completed in a fraction of a second (Card and Dickinson, 2008; Kimmel et al., 1974), while long-term behaviors associated with sexual maturation and circadian rhythm can continue over hours, days, or years (Konopka and Benzer, 1971; Sisk and Foster, 2004; Sokolowski et al., 1984). These timescales interact, so that the probability of responding to an instantaneous stimulus depends on longer-lasting effects of context, learning, motivational states, and age. Our current understanding of the biological basis of behavior arises from well-defined stimulus paradigms that control the environment and experience and from increasingly precise control of genetic

differences between individuals. The endogenous states that modify the effects of genes and the environment on intermediate timescales are less explored. Here, we use long-term behavioral analysis to address two questions: the organization of spontaneous behaviors over development and the existence of individual differences between isogenic animals.

The nematode worm *Caenorhabditis elegans* is ideal for exploring these questions. It is known for its reproducible development, yet even the genetically homogeneous progeny of self-fertilizing hermaphrodites can manifest inter-individual variability. Isogenic animals cultivated under the same conditions vary in life-history traits like the propensity to dauer formation (Fielenbach and Antebi, 2008), longevity (Pincus et al., 2011; Rea et al., 2005), stress response (Casanueva et al., 2012), and the expression of mutant phenotypes (Raj et al., 2010). Whether this variation is stochastic or consistent is difficult to determine, since most of these traits are only measured once per animal.

Intrinsic phenotypic variability in individuals of identical genotypes has been described in a number of species. At the single-cell level, variability in clonal cell populations has been demonstrated in the transformation competence of *Bacillus subtilis* (Süel et al., 2006), in *Tetrahymena* motility (Jordan et al., 2013), and in the apoptosis and cell cycle duration of mammalian cells (Sandler et al., 2015; Spencer et al., 2009). Some of this variation appears to be stochastic and transient, but some persists over a cell's lifetime and even across a few generations (Jordan et al., 2013; Sandler et al., 2015). Similarly, the behavior of several animal species includes reports of consistent individuality that is apparently independent of genetic or environmental causes. For example, the escape responses of pea aphids (Schuett et al., 2011) and the phototaxis and behavioral "handedness" of *Drosophila* (Buchanan et al., 2015; Kain et al., 2012) vary within isogenic populations, with individuals showing consistent behavioral traits over hours or days of testing.

An animal's behavior can be expressed many times over its lifetime, a quality that makes it possible to determine whether one individual within an isogenic population is consistently different from others. Here we monitor the behavior of individual *C. elegans* animals continuously across development using a newly developed multi-camera imaging system to track spontaneous locomotion at high spatiotemporal resolution from hatching to adulthood. These behavioral measurements reveal stereotyped long-term behavioral trajectories across and within

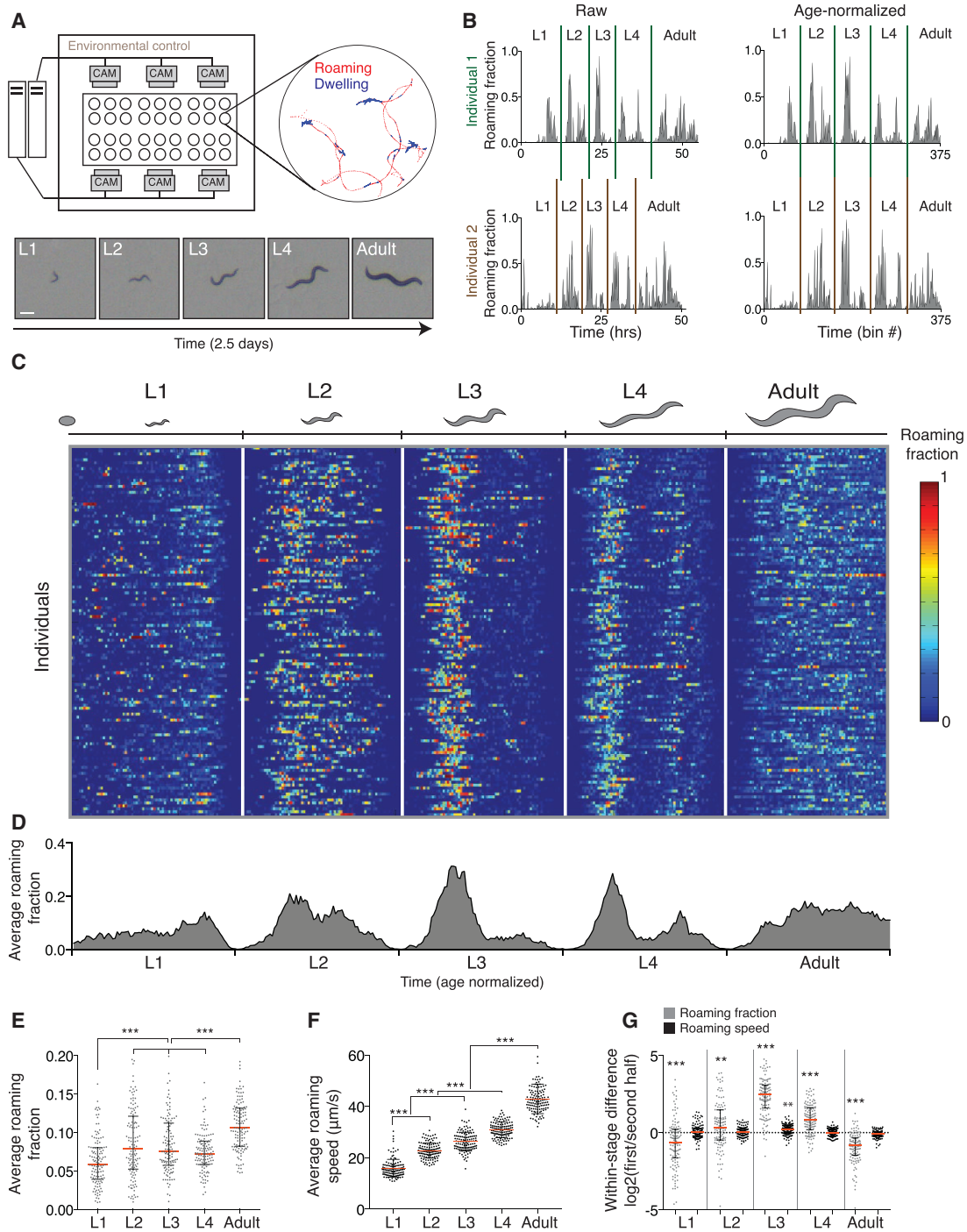


Figure 1. Long-Term Behavioral Tracking of Individual *C. elegans*

(A) (Top left) Multi-camera imaging system for tracking locomotory behavior of single animals across all developmental stages at high spatiotemporal resolution under controlled environmental conditions. Sample 1-hr trajectory shows an animal's location during active roaming states (red) and less active dwelling states (blue); 18% of time in this trajectory was spent roaming. (Bottom) Captured images of animals at different developmental stages; scale bar, 200 μm .

(B) Raw (left) and age-normalized (right) behavioral trajectories for two individuals. Normalization converts each developmental stage into 75 time bins of equal duration ($\sim 6\text{--}12$ min each).

(C) Roaming and dwelling behavior of wild-type N2 individuals across all developmental stages ($n = 125$). Each row in the heatmap shows the age-normalized behavioral trajectory of a single animal. Color represents the fraction of time that the individual spent roaming in each of 375 time bins of the experiment. White lines indicate the midpoint of lethargus during molting. Larval stage durations and additional roaming-dwelling parameters are shown in [Figures S1 and S2](#).

(legend continued on next page)

developmental stages, with characteristic active and less-active periods that last for hours. In addition, we find that a subset of animals expresses consistent behavioral biases across development that distinguish them from isogenic siblings raised under the same conditions. Both the structure of long-term behavior and individual consistency are regulated by neuromodulators that have distinct effects on behavioral outcomes.

RESULTS

C. elegans Has Long-Term Behavioral Patterns within and across Developmental Stages

We tracked behaviors of *C. elegans* individuals grown from egg to adulthood in an environmental chamber with controlled temperature, humidity, and illumination (see [STAR Methods](#) and [Figure 1A](#)). Animals were cultivated in isolation in individual arenas filled with agar and a defined amount of UV-killed OP50 bacterial food to avoid social interactions. An imaging system with an array of cameras captured movies continuously at a frame rate of 3 frames/s and a spatial resolution of $\sim 10 \mu\text{m}$. One camera imaged up to six circular arenas in a custom-made, laser-cut multi-well plate. Using 6 cameras, up to 36 animals per experiment were monitored for ~ 60 hr spanning larval stages L1 to L4 and the first 16 hr of the adult stage, encompassing egg laying that began around 12–14 hr after the final molt. Each experiment captured approximately 650,000 movie frames per animal ([Figure S1A](#) and [Movie S1](#)).

Wild-type animals varied by 10% (37 ± 1.6 [SD] hr) in the time from egg hatching to start of adulthood ([Figure S1B](#)). To minimize this effect and facilitate comparisons between mutant genotypes, we analyzed age-normalized behavioral trajectories aligned to larval stages, defined using the quiescent lethargus behavior of molting animals ([Cassada and Russell, 1975](#)). We then subdivided each larval stage into 75 bins for a total of 375 bins per behavioral trajectory ([Figure 1B](#)).

The behavior of each animal across time was quantified using established parameters for spontaneous foraging states. During locomotion in a food environment, *C. elegans* spontaneously alternates between two foraging states called roaming and dwelling, spending seconds to minutes in each state ([Ben Arous et al., 2009](#); [Flavell et al., 2013](#)). When roaming, the animal explores a large area at a high speed with a low turning rate; when dwelling, the animal explores a smaller area by reducing its speed and increasing its turning rate ([Figure 1A](#)). Although the exact speed and turning rates vary as the animal grows, the distinction between roaming and dwelling is present at all developmental stages ([Figure S1C](#)). Under the conditions used here, roaming states represented 4%–16% of an animal's behavior across development; the parameters we assessed here are the fraction of time spent in the roaming state and the average locomotion speed during roaming states.

Quantification of the wild-type N2 population revealed a stereotyped long-term structure of roaming and dwelling behavior between and within different developmental stages ([Figures 1C](#) and [1D](#)). On average, L1 animals spent the least time roaming. L2, L3, and L4 animals roamed more, but were not significantly different from each other, and adult animals roamed the most ([Figures 1E](#) and [S2A](#)). In addition, each stage had a characteristic behavioral substructure ([Figures 1C](#) and [1D](#)). In the L1 stage, the roaming fraction increased over time. The L2 stage was weakly biphasic, with two blunted peaks of roaming activity. The L3 and L4 stages were strongly biphasic, with abundant roaming in the first half and little roaming in the second half of each stage, albeit with a second small roaming peak in L4. The temporal distinction between the first and second halves of each larval stage was statistically robust ([Figures 1G](#) and [S2D](#)). Adults increased the fraction of time spent roaming over the first 8 hr of adulthood, reaching a steady state for the second 8 hr.

As a second behavioral parameter, we quantified the instantaneous speed of animals in the roaming state. The average wild-type roaming speed increased across all larval stages ([Figures 1F](#) and [S2B](#)). Unlike the fraction of time spent roaming, roaming speed was homogeneous within each larval stage ([Figure 1G](#) and [S2E](#)).

In summary, *C. elegans* varies in the fraction of time spent roaming across and within different developmental stages, with a timescale of hours that is distinct from the minute-long timescale of individual roaming events. Each larval stage is subdivided into characteristic behavioral epochs in its first and second halves, in addition to the brief quiescent periods during molting. This complex roaming trajectory coexists with a stepwise increase of roaming speed at each successive larval stage.

Single Animals Show Consistent Individuality in Behavior

The long-term imaging configuration made it possible to detect substantial variation in the behavior of different individuals. For example, on average, animals spent 9% of the L2 stage roaming, but the range for different individuals was 1%–27% ([Figure S2A](#)). Roaming speed also varied across individuals ([Figure S2B](#)) but less so than the roaming fraction, as indicated by the lower coefficient of variation in this measurement ([Figures S2C](#) and [S2F](#)).

Remarkably, single animals had consistent individual biases in roaming fraction and roaming speed that were sustained across developmental stages. We quantified these biases in behavior over time by ranking each individual against the entire population ($n = 125$) in 50 time bins representing the complete developmental trajectory. The rank approach allowed a unified comparison of behavior that corrects for its heterogeneity over developmental time. The distribution of rank scores across the time course was then analyzed to yield a normalized consistency index that is positive for animals that consistently roam more

(D) Average fraction of time roaming in the population.

(E) Average fraction of time roaming of individuals in each stage.

(F) Average roaming speed of individuals in each stage.

(G) Comparison of the first and second half of each stage (L1 to adult), calculated for each individual as $\log_2(\text{behavior in } 1^{\text{st}} \text{ half}/\text{behavior in } 2^{\text{nd}} \text{ half})$.

In (E–G), each point represents an animal, red bars represent population mean, and black bars represent Q1–Q3 range. Statistical significance values were calculated using Wilcoxon rank test. ** $p < 0.01$, *** $p < 0.001$. See also [Movies S1](#) and [S2](#).

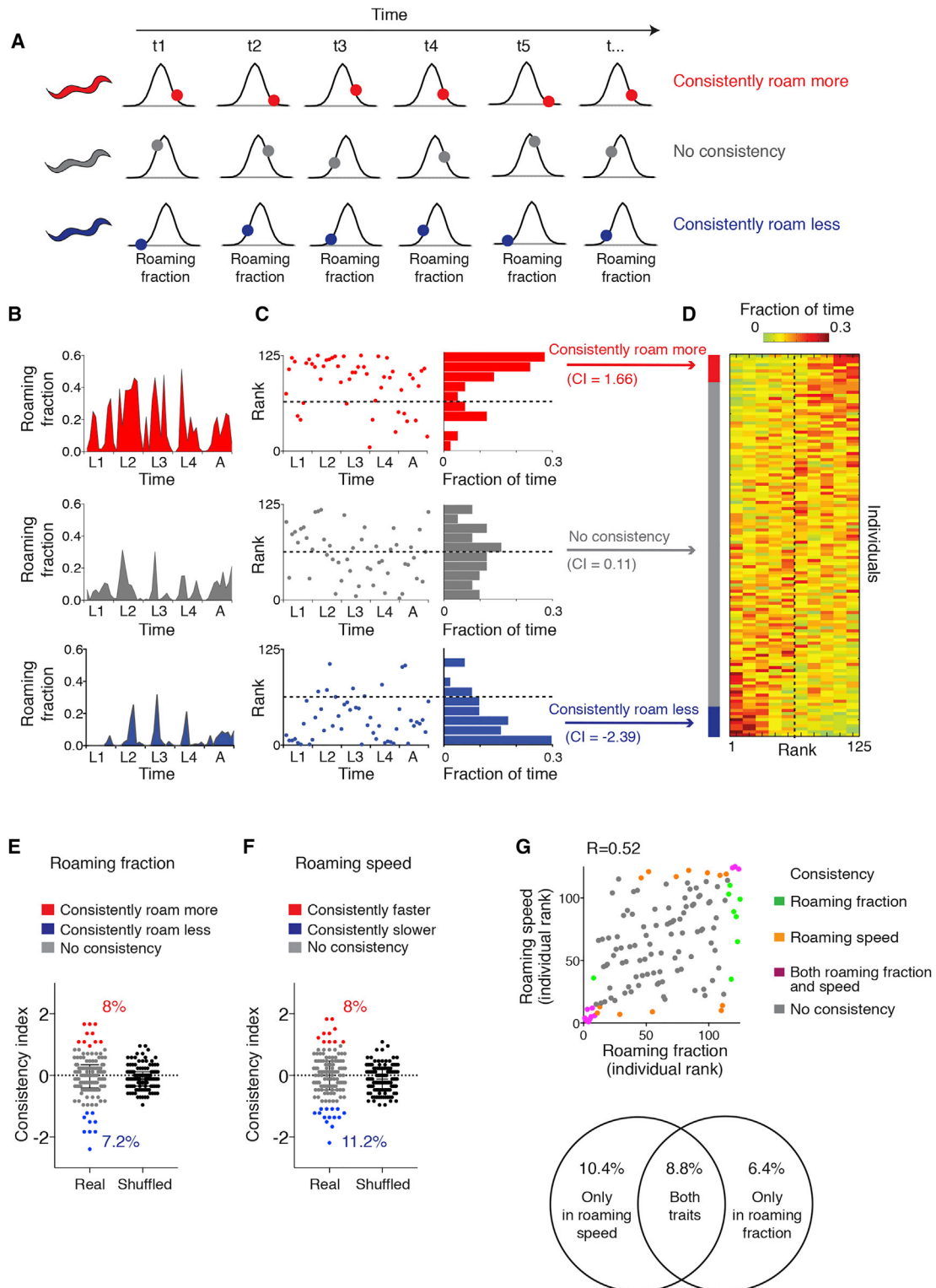


Figure 2. Single Animals Show Long-Term Individuality in Behavior

(A) Schematic illustrating individuality in behavior. Animals showing consistent individuality roam more (red) or less (blue) relative to the population median at many time points, whereas animals that do not show individuality (gray) do not show consistency over time.

(B) Examples of three wild-type N2 individuals from the datasets that consistently roamed more (red), roamed less (blue), or did not show consistent individuality in roaming (gray).

(legend continued on next page)

than the median in many time bins, negative for animals that consistently roam less, and close to zero for animals that do not show significant consistency in their behavior (Figures 2A–2D and Movie S2). Over the course of development, a significant fraction of animals showed individual bias in behavior: 8% of the animals consistently roamed more and 7.2% consistently roamed less than expected based on a shuffled dataset (Figure 2E).

A similar developmentally normalized rank analysis of the average speed during roaming episodes showed that 8% of animals were consistently faster and 11.2% were consistently slower than expected in a shuffled dataset (Figure 2F). The animals with significant consistency in both roaming fraction and roaming speed overlapped more than expected by chance, but not entirely (Figure 2G). Differences in behavior between individuals were not heritable; populations grown from animals that showed extreme but opposite individual bias returned to the average population behavior (Figure S3).

These results indicate that a subset of *C. elegans* animals of the same genotype in a common environment express long-term individual bias in behavior compared to the population and further indicate that different individuals can express consistent bias in different behavioral traits.

Neuromodulators Control Long-Term Behavioral Structure within and across Stages

A variety of genes are known to affect *C. elegans* roaming fraction or roaming speed over timescales of seconds to minutes (Ben Arous et al., 2009; Flavell et al., 2013; Fujiwara et al., 2002; Greene et al., 2016; Sawin et al., 2000; Shtonda and Avery, 2006). Prominent among the implicated molecules are small-molecule biogenic amines and neuropeptide systems (Alkema et al., 2005; Chase and Koelle, 2007; Sulston et al., 1975; Sze et al., 2000), which regulate behavior by modulating G protein-coupled biochemical pathways, protein phosphorylation, and gene expression, as well as neuronal excitability. To ask whether neuromodulation regulates long-term patterns of behavior across development, we examined a number of genes that affect adult roaming fraction or roaming speed using long-term behavioral tracking (Figure 3 and Movie S3).

Animals that lack serotonin due to a mutation in the biosynthetic enzyme tryptophan hydroxylase (TPH-1) roam more than

wild-type animals as adults (Flavell et al., 2013). We found that the roaming fraction was consistently increased in *tph-1* mutants across all developmental stages (Figures 3, 4A, and S4A). Despite this general scaling effect, the long-term trajectory of behavior within and between larval stages was preserved in *tph-1* mutants. Like wild-type animals, *tph-1* mutants roamed more in the first half of the L2–L4 stages than in the second half of each stage and less in the first half of L1 and early adult stages than in the second half (Figures 4A and S4C).

Like *tph-1* mutants, animals mutant for the neuropeptide receptor NPR-1 roam more than wild-type animals as adults (Cheung et al., 2005). *npr-1* mutants also have a reduction in quiescent behavior during molting (Choi et al., 2013) (Figure 4B). We found that *npr-1* mutants roamed more than the wild-type at all larval stages (Figures 4B and S4A) and that in addition, the behavioral trajectory within larval stages was highly abnormal. For example, *npr-1* animals had much higher roaming fractions in the first half than in the second half of the L1 stage, the opposite pattern from wild-type (Figures 4B and S4F). *npr-1* roaming trajectories within other stages were also distinct from the wild-type; for example, the suppression of roaming in the second half of the L3 and L4 stages was reduced (Figures 4B and S4F). *npr-1* mutants are hypersensitive to the arousing effects of environmental oxygen (Cheung et al., 2005); the effects of the mutation suggest that these arousing effects override the typical developmental pattern.

The transforming growth factor (TGF)- β mutant *daf-7* roams less than wild-type in the adult stage (Ben Arous et al., 2009). We found that its effects were discontinuous across developmental stages: *daf-7* animals roamed more than wild-type in the L2 stage and less in all other stages (Figures 4C and S4A). In addition, they lacked the roaming peak in the first half of the L3 and L4 stages (Figures 4C and S4G). *daf-7* alters the developmental propensity to form an alternative larval stage called a dauer larva (Riddle et al., 1981), but this effect was set aside by analyzing only animals that did not enter the dauer stage (58% of all animals under these conditions). Among the mutants studied here, only *daf-7* altered developmental timing as well as behavior—the duration of the L1 and L2 stages was extended in all *daf-7* larvae, consistent with broader metabolic and developmental effects of *daf-7* (Figure S5A) (Wadsworth and Riddle, 1989).

(C) Rank in the population over time for individuals in (B) assessed by dividing the trajectory into 50 time bins (10 per stage, ~ 1 hr each; 125 roamed the most, 1 dwelled the most, dashed lines indicate median), and histogram of ranks of the individual across all time points. Consistency index (CI) of each individual is indicated.

(D) Rank distributions (as in C, right, rotated 90° clockwise) for all N2 individuals ($n = 125$) sorted by their consistency index (top to bottom, positive to negative consistency index, respectively).

(E) Roaming fraction consistency in wild-type individuals that show significant positive roaming consistency (consistently roam more, red), significant negative roaming consistency (consistently roam less, blue), or no consistency (gray) compared to shuffled dataset of the same number of individuals (black). Statistical significance was calculated for each individual by bootstrapping (false discovery rate [FDR, adjusted p value] < 0.05). The consistent behavioral bias appears not to be heritable (Figure S3). Black bars represent Q1–Q3 range.

(F) Roaming speed consistency in wild-type individuals that show significant positive roaming speed consistency (consistently faster, red), significant negative roaming speed consistency (consistently slower, blue), or no consistency (gray) compared to shuffled dataset of the same number of individuals (black). Statistical significance was calculated for each individual by bootstrapping (FDR [adjusted p value] < 0.05). Black bars represent Q1–Q3 range.

(G) (Top) Plot showing all animals in the N2 population and their respective roaming fraction and roaming speed ranks in the population. Animals showing significant consistency in roaming fraction only (green), in roaming speed only (orange), or in both traits (magenta) are marked. Correlation coefficient (R) represents the Pearson correlation between roaming speed and roaming fraction ranks in individuals. (Bottom) Overlap between subpopulations showing significant consistency in roaming fraction and roaming speed.

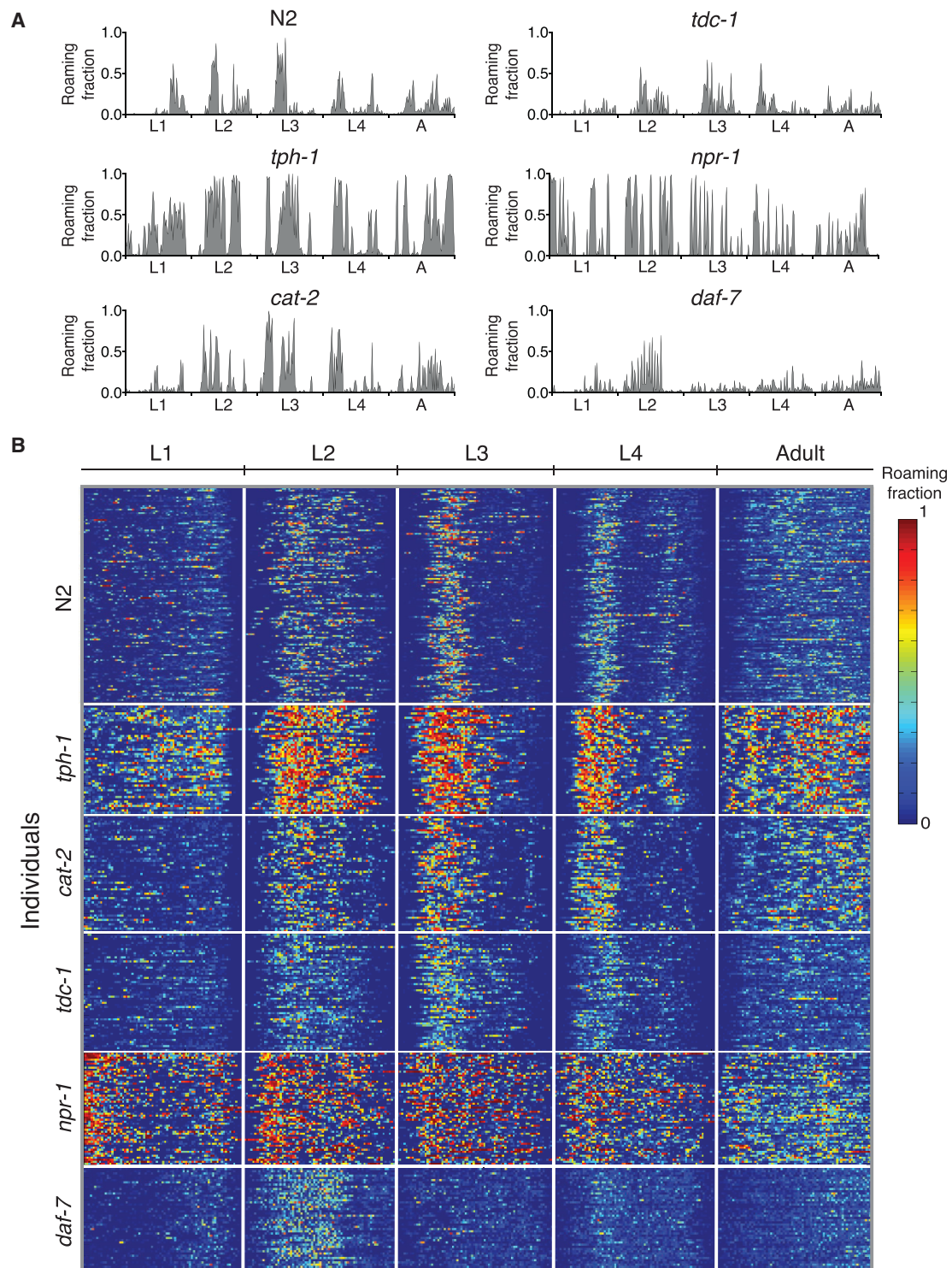


Figure 3. Long-Term Behavioral Tracking of Neuromodulatory Mutants

Mutants are *tph-1*, which encodes a tryptophan hydroxylase needed for serotonin synthesis; *cat-2*, which encodes a tyrosine hydroxylase needed for dopamine synthesis; *tdc-1*, which encodes a tyrosine decarboxylase needed for tyramine and octopamine synthesis; *npr-1*, which encodes a neuropeptide receptor in the neuropeptide Y receptor family; and *daf-7*, which encodes a secreted TGF- β -related protein.

(A) Representative individual age-normalized behavioral trajectories.

(legend continued on next page)

Roaming speed was also regulated by neuromodulators across development but in a distinct genetic and temporal pattern compared to roaming fraction. *npr-1* neuropeptide receptor mutants had elevated roaming speeds at all stages (Figures 4D and S4B), but other neuromodulators showed time-dependent effects. Both *tph-1* serotonin-deficient mutants and *cat-2* dopamine-deficient mutants were indistinguishable in roaming speed from wild-type in the L1 stage but faster in all subsequent stages (Figures 4D and S4B). *daf-7* TGF- β mutants had a higher roaming speed than the wild-type in the L2, L4, and adult stages, but not in the L3 (Figures 4D and S4B).

Following the observation that *cat-2* dopamine mutants have increased variability in locomotion speed in the adult stage (Sawin et al., 2000; Omura et al., 2012), we also examined speed variability during roaming episodes (Figures S4H and S4I). Variability was scored at the individual animal level using the coefficient of variation, a scale-free parameter. The effect of *cat-2* on speed variability began in the L2 stage and increased in subsequent stages (Figures S4H and S4I). A reciprocal pattern was present in *daf-7* mutants, which had increased roaming speed variability in the L1–L3 stages and normal variability in the L4 and adult stages. Although *tph-1* had a large effect on roaming speed, it did not affect variability. Significant changes in speed variability were also observed in *npr-1* mutants and in *tdc-1* animals deficient in tyramine and octopamine synthesis (Figures S4H and S4I).

In conclusion, the separate evaluation of roaming fraction, roaming speed, and speed variability identify highly heterogeneous effects of neuromodulators on time-dependent behavioral dynamics.

Neuromodulation Regulates Individuality in Behavior

To ask if neuromodulators can also control individuality in behavior, we quantified the behavioral consistency of mutant animals across different developmental stages.

Strikingly, *tph-1* serotonin-deficient animals appeared to lack any consistent individuality in roaming fraction, whereas 15.2% of wild-type animals had a consistent bias to roam either more or less than the population average (Figures 4E and S5B). The decrease in apparent individuality could not be explained purely as a ceiling effect of increased roaming fraction in *tph-1* mutants, as *npr-1* individuals had a similar increase in roaming fraction (Figure 4B), with no change in consistent individuality (Figures 4E and S5B). *cat-2*, *tdc-1*, and *daf-7* mutants were also similar to the wild-type (Figures 4E and S5B).

Consistent individuality in roaming speed had a distinct pattern of genetic regulation. *tdc-1* tyramine- and octopamine-deficient mutants, *npr-1* neuropeptide receptor mutants, and *daf-7* TGF- β mutants all had a higher fraction of animals with a consistent bias toward high or low roaming speeds (Figures 4F and S5C). *tph-1* serotonin mutants and *cat-2* dopamine mutants were not significantly different from wild-type (Figures 4F and

S5C). These results indicate that specific neuromodulators can either increase or buffer long-term individuality in behavioral traits.

Serotonin Receptors Show Unique Effects on Long-Term Behavior and Individuality

The dual role of serotonin in regulating long-term roaming patterns and consistent individuality prompted a closer examination of serotonin signaling. We first asked whether increased serotonin levels affected roaming. Animals mutant for the *mod-5* serotonin reuptake transporter, which terminates serotonin signaling, roamed less than wild-type animals during all developmental stages (Figures 5 and 6A). The opposite effects of serotonin depletion (*tph-1*) and excess serotonin accumulation (*mod-5*) suggest that serotonin instructively determines the fraction of time spent roaming across development.

C. elegans has five characterized serotonin receptors: the G protein-coupled metabotropic receptors SER-1, SER-4, SER-5, and SER-7 (Carre-Pierrat et al., 2006; Hamdan et al., 1999; Hobson et al., 2003; Olde and McCombie, 1997), and a serotonin-gated chloride channel (MOD-1) (Ranganathan et al., 2000). No single serotonin receptor recapitulated all of the effects of *tph-1* on roaming fraction. Instead, the receptor mutants revealed developmental heterogeneity in serotonin signaling that was not evident from its complete removal in a *tph-1* mutant (Figures 5, 6B–6E, and S6A). Thus *ser-1* animals roamed more during the L1–L3 stages but resembled the wild-type in L4 and adult stages (Figures 6B and S6A). Conversely, *ser-7* animals roamed more than the wild-type only as adults (Figures 6C and S6A). *ser-4* had a small but significant increase in roaming during L4 and adult stages (Figure 6D). Animals lacking the serotonin-gated chloride channel MOD-1 were intermediate between wild-type and *tph-1* at all stages (Figures 6E and S6A). *ser-5* mutants had minimal effects (Figures 6D and S6A).

The effects of serotonin receptor mutants on roaming speed largely overlapped with their effects on roaming fraction (Figure S6B). *mod-1* mutants had increased roaming speed from the L2 to the adult stages, like *tph-1* mutants, but with a smaller effect magnitude. *ser-1* mutants had increased roaming speed in L2 and L4 stages, *ser-4* mutants in L4 and adult stages, and *ser-7* only as adults. The serotonin reuptake transporter *mod-5* significantly decreased roaming speed in L2, L3, and adult stages, consistent with an instructive effect.

Next, we examined the effects of altered serotonin signaling on consistent individuality. *mod-5* mutants with enhanced serotonin signaling had an increased level of consistent individuality in roaming fraction, opposite to *tph-1* mutants (Figures 6F and S6C). This result suggests that behavioral individuality is associated with dose-dependent effects of serotonin. Among the serotonin receptors, *ser-4* mutants had a sharp decrease in consistent individuality, like *tph-1* mutants (Figures 6F and S6F). No other serotonin receptor mutant was significantly

(B) Roaming and dwelling behavior in all mutant and wild-type individuals, age normalized. Each row in the heatmap shows the behavioral trajectory of a single animal. Color represents the fraction of time that the individual spent roaming in each of 375 time bins along the experiment (N2, n = 125; *tdc-1*, n = 57; *cat-2*, n = 53; *tph-1*, n = 48; *npr-1*, n = 56; *daf-7*, n = 46). Further analysis of roaming parameters appears in Figure S4. *daf-7* mutants have prolonged L1 and L2 stages; developmental timing in all other mutants resembles the wild-type (Figure S5). See also Movie S3.

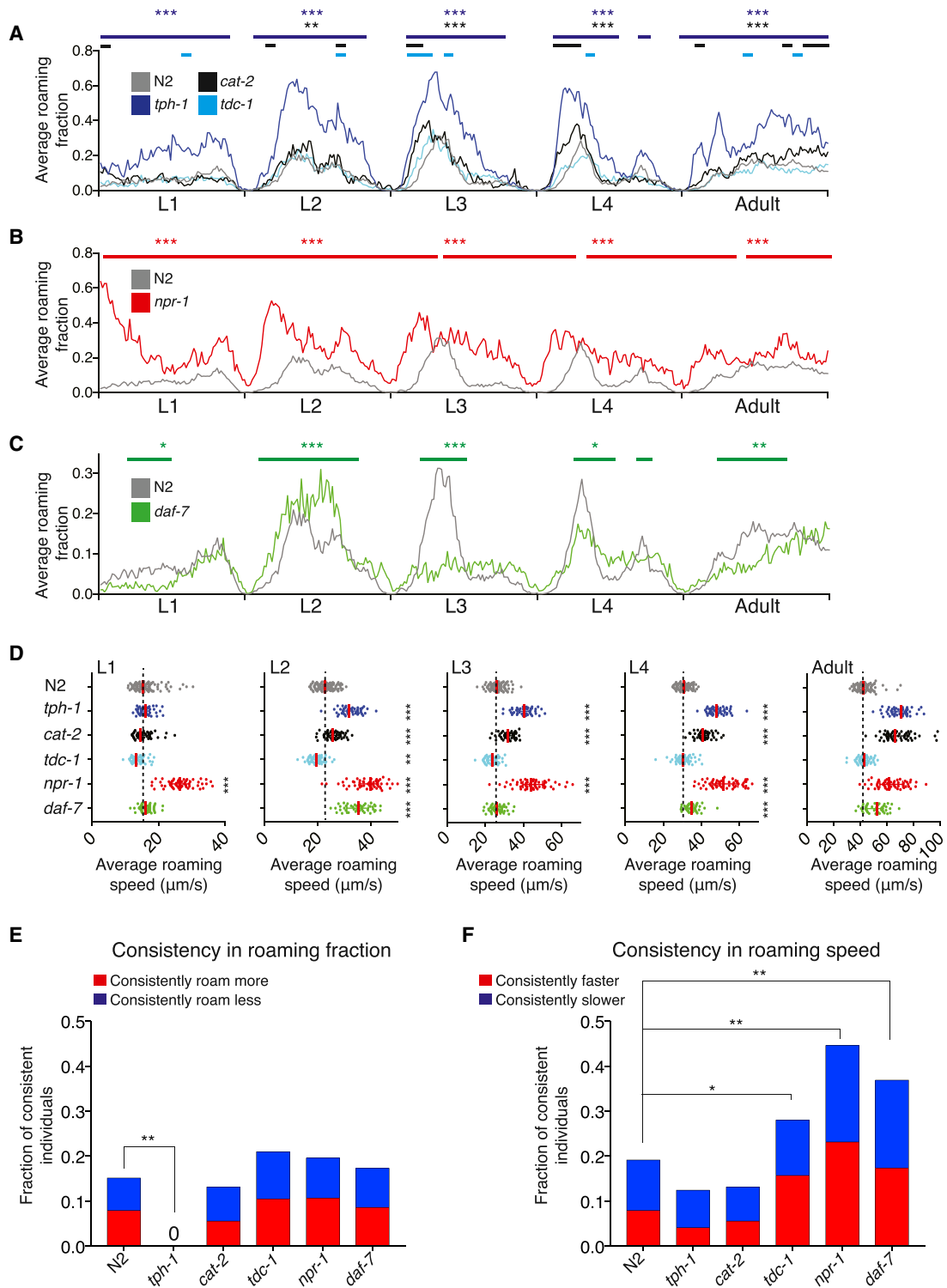


Figure 4. Neuromodulatory Effects on Behavioral Trajectories and Consistent Individuality

(A–C) Average fraction of time roaming across all developmental stages of mutants and wild-type animals. (A) Biogenic amine mutants. (B) *npr-1* neuropeptide receptor mutants. (C) *daf-7* TGF- β mutants. Upper bars represent time periods in which mutant behavior was significantly different from wild-type behavior ($p < 0.01$, Jensen-Shannon (JS) divergence, FDR corrected). Upper asterisks represent the significance of the overall difference between the mutant and wild-type in each developmental stage (1 bin per stage). * $p < 0.05$, ** $p < 0.01$, *** $p < 0.001$ (FDR corrected).

(legend continued on next page)

different from the wild-type (Figures 6F, S6D, S6E, S6G, and S6H). Thus, serotonin receptor mutants separate the effects of serotonin on roaming fraction and its effects on behavioral individuality and partition the effects of serotonin across development.

DISCUSSION

Behavior results from a combination of endogenous properties of the nervous system and reactive responses to external stimuli. By focusing on spontaneous behavior, we examine how endogenous properties of the nervous system change over time during development. Our analysis shows that *C. elegans* behavior is partitioned into many temporal and developmental windows, each lasting for hours and each susceptible to unique neuromodulatory controls. In addition, we show that isogenic animals in the same environment can have a consistent behavioral bias that differs from the population average, and we further implicate neuromodulatory mechanisms as instructive regulators of this process.

Long-term behavioral traits in many animals are mediated by secreted endocrine or peptide factors: secreted steroid hormones and neuropeptides in mammalian puberty (Sisk and Foster, 2004), ecdysis hormones and neuropeptides in insect developmental transitions (Truman, 2005; Wigglesworth, 1936), and the neuropeptides pigment-dispersing factor (PDF) and vasoactive intestinal peptide (VIP) in invertebrate and vertebrate circadian behaviors (Aton et al., 2005; Park and Hall, 1998). We show here that locomotory behavior of *C. elegans* has reproducible, dynamic long-term structure across and within different developmental stages. Individual larval stages, and even the first and second half of each larval stage, have stereotyped properties implying the existence of an innate template for behavior across development. *C. elegans* was previously known to have a sleep-like lethargus state during molting (Raizen et al., 2008), but was not known to have structured within-stage activity patterns. Interestingly, *C. elegans* metabolic gene expression changes cyclically within each larval stage (Hendriks et al., 2014). It might be informative to determine whether metabolic and behavioral changes within stages are controlled by common biological inputs or whether they affect each other.

Building on their known effects on adult roaming behavior and locomotion speed, we identified neuromodulators that can affect developmental stage-specific behavior. Some effects were developmentally smooth: dopamine-deficient mutations affected roaming speed more during later developmental stages, but left the overall trajectory of stage-specific behaviors intact. Other effects were discontinuous: *daf-7* mutations had opposite effects on roaming fraction in L2 versus L3–adult stages, and

eliminated the characteristic biphasic roaming trajectory within L3 and L4 stages. *npr-1* mutations altered within-stage trajectories of every developmental stage. The unique behavioral effects of each gene suggest that neuromodulators generate temporal behavioral heterogeneity at multiple timescales.

Further developmental heterogeneity was uncovered by a detailed examination of serotonin signaling. Serotonin is a key regulator of animal behavior and metabolism and interacts with many receptors in each species (Dempsey et al., 2005; Ranganathan et al., 2000; Saudou et al., 1994; Song et al., 2013; Witz et al., 1990; Yeh et al., 1996). In *C. elegans*, a complete depletion of serotonin (*tph-1*) resulted in increased roaming across development, but the serotonin receptor mutants partitioned roaming by stages, with *ser-1* acting in the first three larval stages, *ser-4* in the L4 and adult stages, and *ser-7* in adults. SER-1, SER-4, and SER-7 are G protein-coupled receptors that resemble the mammalian 5HT2, 5HT1, and 5HT7 receptors, respectively (Hamdan et al., 1999; Gürel et al., 2012; Hobson et al., 2003; Song et al., 2013). Each is expressed in a number of neurons, and SER-7 is also expressed in muscles and the intestine. The overlap in their reported expression patterns is minimal, and in addition, they couple through different signaling pathways—SER-1 through Gq (*egl-30*), SER-4 through Go (*goa-1*), and SER-7 through Gs (*gsa-1*). MOD-1, a serotonin-gated chloride channel that acts in a number of neurons, affected roaming fraction at all stages, although to a lesser extent than *tph-1* (Ranganathan et al., 2000; Flavell et al., 2013).

These first-level genetic studies leave many open questions about the roles of specific modulators and receptors across development. Importantly, the cellular sites at which the genes act to affect these behaviors are unknown. In addition, only one mutant allele was examined per gene, so subtle effects could have been exaggerated or suppressed by background mutations.

Developmentally regulated behaviors are widespread in animals, including humans. Our results add to the evidence that even behaviors that are observed across development can switch their patterns of neuromodulatory control. In one previous example, the stomatogastric ganglion of the lobster, which controls feeding rhythms throughout life, changes both its expression of neuropeptides and its sensitivity to those neuropeptides during development (Rehm et al., 2008). These observations might suggest mechanisms for known developmental changes in mammalian behavior and pharmacology. For example, fear-extinction learning in both humans and mice is suppressed during adolescence compared to earlier and later ages (Pattwell et al., 2012), suggesting a change in its regulation over time. With respect to serotonin, the reuptake inhibitor fluoxetine (Prozac) has different effects on motivated behaviors in

(D) Average roaming speed of mutant individuals compared to wild-type individuals across developmental stages. Each point represents an animal, red bars represent population mean, dashed line indicates the average of the N2 population in each stage. ** $p < 0.01$, *** $p < 0.001$ (JS divergence, FDR corrected).

(E) Fraction of mutant individuals that showed significant positive roaming consistency (consistently roam more, red) or significant negative roaming consistency (consistently roam less, blue).

(F) Fraction of mutant individuals that showed significant positive roaming speed consistency (consistently faster, red) or significant negative roaming speed consistency (consistently slower, blue). Statistical significance values of differences between the fractions of consistent individuals in different genotypes were calculated using bootstrapping. * $p < 0.05$, ** $p < 0.01$ (FDR corrected).

See also Figure S4. Further analysis of behavioral consistency appears in Figure S5.

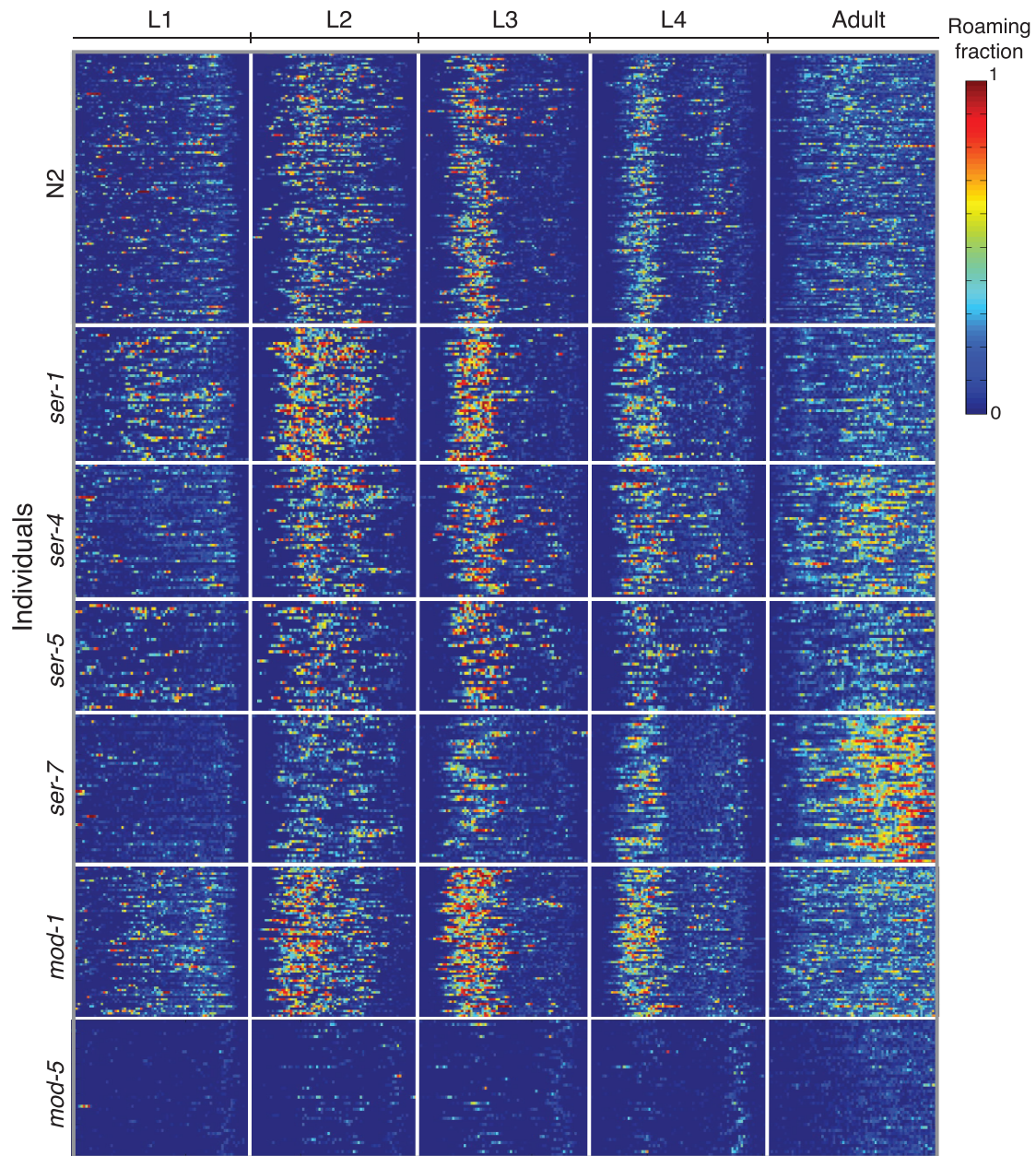


Figure 5. Long-Term Behavioral Tracking of Serotonin Receptor and Serotonin Reuptake Transporter Mutants

Roaming and dwelling behavior in serotonin receptors mutants (*ser-1*, n = 50; *ser-4*, n = 50; *ser-5*, n = 36; *ser-7*, n = 53; *mod-1*, n = 65), serotonin reuptake transporter mutants (*mod-5*, n = 45), and wild-type individuals (N2, n = 125), age normalized. Each row in the heatmap shows the behavioral trajectory of a single animal. Color represents the fraction of time that the individual spent roaming in each of 375 time bins along the experiment. See also Figure S6.

adolescent and adult hamsters (Shannonhouse et al., 2016), and the use of this class of compounds in human adolescents has raised concerns (Jane Garland et al., 2016). Our studies suggest that examining the developmental regulation of behavior by neuromodulatory systems is a promising area for further exploration.

Stable differences in individual behavior are generally described as resulting either from genetic variation (de Bono

and Bargmann, 1998; Sokolowski, 1980) or from different life experiences such as imprinting (Jin et al., 2016; Lorenz, 1935). The consistent behavioral individuality we observe in *C. elegans* is apparently neither genetic nor environmental. Individuality in behavior among genetically and environmentally matched adult animals has also been demonstrated in flies and pea aphids (Buchanan et al., 2015; Kain et al., 2012; Schuett et al., 2011). From an evolutionary point of view, the generation of phenotypic

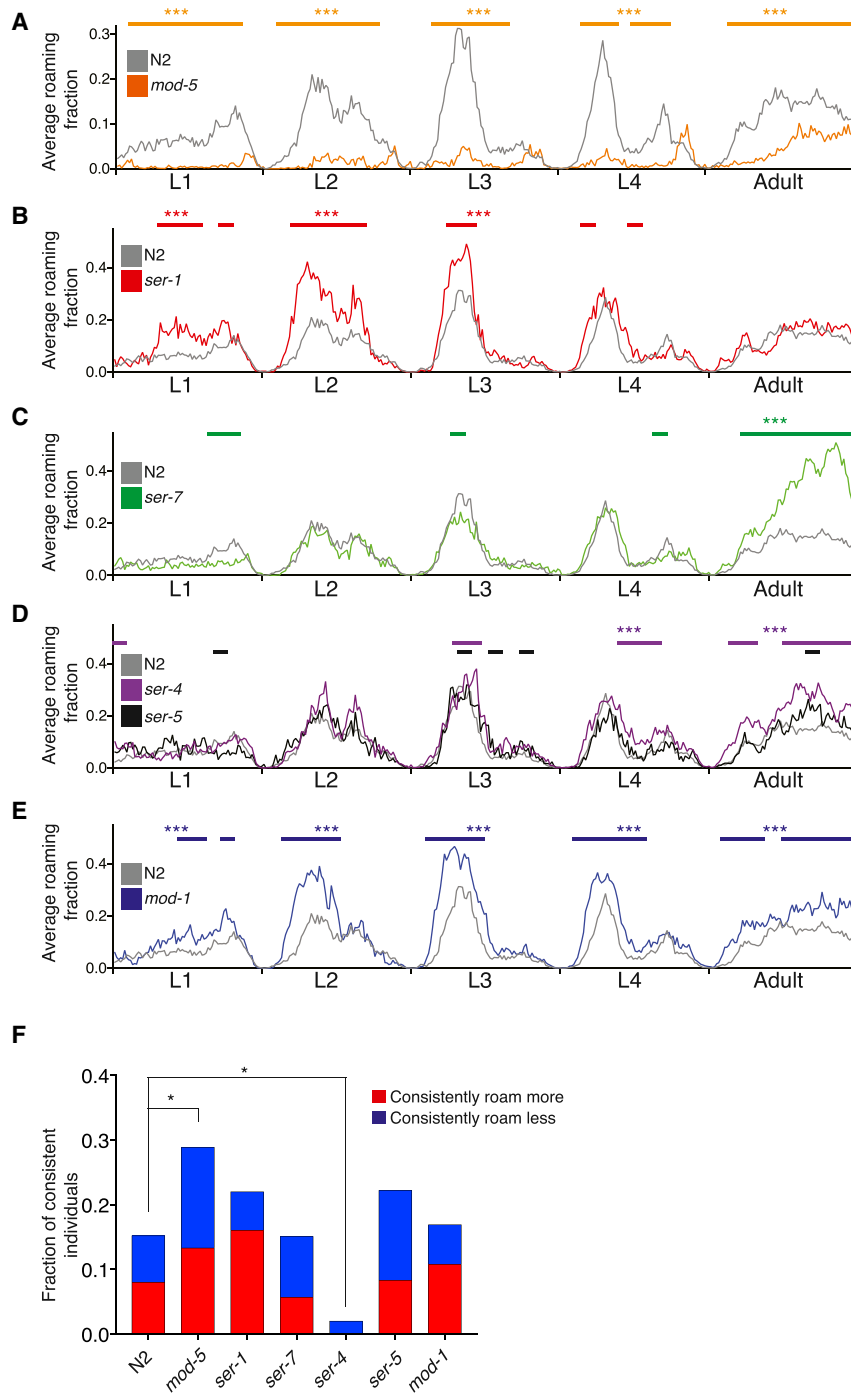


Figure 6. Serotonin Receptor Mutants Partition Behavioral Effects across Development

(A) Average fraction of time roaming across all developmental stages of *mod-5* serotonin reuptake transporter mutants and wild-type N2 animals. (B–E) Average fraction of time roaming across all developmental stages of serotonin receptor mutants and wild-type N2 animals. Upper bars represent time periods in which mutant behavior was significantly different from wild-type behavior ($p < 0.01$, JS divergence, FDR corrected). Upper asterisks represent the significance of the overall difference between the mutant and wild-type in each developmental stage (1 bin per stage). *** $p < 0.001$ (FDR corrected). (F) Fraction of mutant individuals that showed significant positive roaming consistency (consistently roam more, red) or significant negative roaming consistency (consistently roam less, blue). Statistical significance values of differences between the fractions of consistent individuals in different genotypes were calculated using bootstrapping. * $p < 0.05$ (FDR corrected). Further analysis of roaming parameters appears in Figure S6.

affecting the left-right asymmetry of an olfactory neuron pair (Troemel et al., 1999). Another candidate source of individuality is variation in epigenetic states among individuals (Mello and Conte, 2004; Rakyan et al., 2002; Weksberg et al., 2002; Wenzel et al., 2011; Wong et al., 2005).

We found that several neuromodulators affect consistent behavioral individuality in *C. elegans*, either increasing (serotonin) or buffering (tyramine/octopamine, NPR-1, DAF-7) the fraction of strongly biased animals in an isogenic population. Serotonin appears to have a dose-dependent effect, as mutations that reduce or increase serotonin result in reciprocal decreases and increases in the fraction of animals showing behavioral consistency. Serotonin also regulates individuality in phototactic behavior in adult flies, where it acts to reduce “personality” (Kain et al., 2012). It is notable that both flies and worms associate serotonin with individual bias in behavior, although its effects are opposite in the two species.

variability among individuals has been proposed to play an adaptive role in unpredictable environments (Cooper and Kaplan, 1982; Slatkin, 1974). The lack of heritability of these effects indicates that non-deterministic processes may generate stable individual-to-individual differences in behavior. Stochastic developmental variability is one biologically plausible mechanism to generate individuality. For example, normal *C. elegans* neuronal development is subject to a stochastic process

Among the serotonin receptor mutants, *ser-4* had a strong effect on behavioral consistency but a relatively mild effect on overall behavioral trajectories. Although less characterized here, the tyramine/octopamine-deficient mutant *tdc-1* also appears to affect individual behavioral consistency without large effects on average behavior. Neuromodulators are well-established regulators of dynamic behavioral states (Rehm et al., 2008); our results suggest that they also contribute to stable

behavioral individuality that arises from stochastic sources. The underlying mechanism of individuality is unknown, but one possibility is that cross-regulatory interactions among neuromodulators can result in a range of stable set points in different animals (Chang et al., 2006; Entchev et al., 2015).

This analysis addresses just a few of the behaviors of *C. elegans*, and there are many additional discoveries to be made using a long-term imaging approach. The complex animal behaviors that are most deeply understood, such as birdsong, are those in which behaviors are measured precisely over long time periods (Doupe and Kuhl, 1999; Nottebohm, 1968). The relationship between long timescales and shorter ones, as for example represented in short, stereotyped behavioral modules in *C. elegans* (Schwarz et al., 2015) and mouse pose dynamics (Wiltchko et al., 2015), provides opportunities for increased depth of analysis (Anderson and Perona, 2014). Such experiments open a new window for understanding the mechanisms generating lifelong behavior and individuality.

STAR★METHODS

Detailed methods are provided in the online version of this paper and include the following:

- KEY RESOURCES TABLE
- CONTACT FOR REAGENT AND RESOURCE SHARING
- EXPERIMENTAL MODEL AND SUBJECT DETAILS
 - *C. elegans* strains
 - Growth conditions
- METHOD DETAILS
 - Imaging system
 - Behavioral trajectory extraction from imaging data
 - Heritability experiments
- QUANTIFICATION AND STATISTICAL ANALYSES
 - Quantification of behavioral parameters
 - Quantification of behavioral individuality
 - Quantification of differences in behavior between genotypes
- DATA AND SOFTWARE AVAILABILITY

SUPPLEMENTAL INFORMATION

Supplemental Information includes six figures and three movies and can be found with this article online at <https://doi.org/10.1016/j.cell.2017.10.041>.

AUTHOR CONTRIBUTIONS

S.S. and C.I.B. designed experiments. S.S. conducted experiments. S.S., C.K., and C.I.B. analyzed and interpreted data, and S.S. and C.I.B. wrote the paper.

ACKNOWLEDGMENTS

We thank the *Caenorhabditis* Genetics Center (CGC) for strains; David Jordan, Stanislas Leibler, Steve Flavell, and Alejandro Lopez for advice and discussions; and the members of our laboratory for comments on the manuscript. C.K. was supported by the Kavli Foundation. S.S. was supported by the EGL Charitable Foundation and the Human Frontiers Science Program (LT000933/2014). This work was supported by the Howard Hughes Medical Institute, of which C.I.B. was an investigator.

Received: May 13, 2017
Revised: September 10, 2017
Accepted: October 24, 2017
Published: November 30, 2017

REFERENCES

- Alkema, M.J., Hunter-Ensor, M., Ringstad, N., and Horvitz, H.R. (2005). Tyramine Functions independently of octopamine in the *Caenorhabditis elegans* nervous system. *Neuron* 46, 247–260.
- Anderson, D.J., and Perona, P. (2014). Toward a science of computational ethology. *Neuron* 84, 18–31.
- Aton, S.J., Colwell, C.S., Harmar, A.J., Waschek, J., and Herzog, E.D. (2005). Vasoactive intestinal polypeptide mediates circadian rhythmicity and synchrony in mammalian clock neurons. *Nat. Neurosci.* 8, 476–483.
- Ben Arous, J., Laffont, S., and Chatenay, D. (2009). Molecular and sensory basis of a food related two-state behavior in *C. elegans*. *PLoS ONE* 4, e7584.
- Buchanan, S.M., Kain, J.S., and de Bivort, B.L. (2015). Neuronal control of locomotor handedness in *Drosophila*. *Proc. Natl. Acad. Sci. USA* 112, 6700–6705.
- Card, G., and Dickinson, M.H. (2008). Visually mediated motor planning in the escape response of *Drosophila*. *Curr. Biol.* 18, 1300–1307.
- Carre-Pierrat, M., Baillie, D., Johnsen, R., Hyde, R., Hart, A., Granger, L., and Ségalat, L. (2006). Characterization of the *Caenorhabditis elegans* G protein-coupled serotonin receptors. *Invert. Neurosci.* 6, 189–205.
- Casanueva, M.O., Burga, A., and Lehner, B. (2012). Fitness trade-offs and environmentally induced mutation buffering in isogenic *C. elegans*. *Science* 335, 82–85.
- Cassada, R.C., and Russell, R.L. (1975). The dauerlarva, a post-embryonic developmental variant of the nematode *Caenorhabditis elegans*. *Dev. Biol.* 46, 326–342.
- Chang, A.J., Chronis, N., Karow, D.S., Marletta, M.A., and Bargmann, C.I. (2006). A distributed chemosensory circuit for oxygen preference in *C. elegans*. *PLoS Biol.* 4, e274.
- Chase, D.L., and Koelle, M.R. (2007). Biogenic amine neurotransmitters in *C. elegans* (WormBook), pp. 1–15.
- Cheung, B.H.H., Cohen, M., Rogers, C., Albayram, O., and de Bono, M. (2005). Experience-dependent modulation of *C. elegans* behavior by ambient oxygen. *Curr. Biol.* 15, 905–917.
- Choi, S., Chatzigeorgiou, M., Taylor, K.P., Schafer, W.R., and Kaplan, J.M. (2013). Analysis of NPR-1 reveals a circuit mechanism for behavioral quiescence in *C. elegans*. *Neuron* 78, 869–880.
- Cooper, W.S., and Kaplan, R.H. (1982). Adaptive “coin-flipping”: a decision-theoretic examination of natural selection for random individual variation. *J. Theor. Biol.* 94, 135–151.
- de Bono, M., and Bargmann, C.I. (1998). Natural variation in a neuropeptide Y receptor homolog modifies social behavior and food response in *C. elegans*. *Cell* 94, 679–689.
- Dempsey, C.M., Mackenzie, S.M., Gargus, A., Blanco, G., and Sze, J.Y. (2005). Serotonin (5HT), fluoxetine, imipramine and dopamine target distinct 5HT receptor signaling to modulate *Caenorhabditis elegans* egg-laying behavior. *Genetics* 169, 1425–1436.
- Doupe, A.J., and Kuhl, P.K. (1999). Birdsong and human speech: common themes and mechanisms. *Annu. Rev. Neurosci.* 22, 567–631.
- Entchev, E.V., Patel, D.S., Zhan, M., Steele, A.J., Lu, H., and Ch’ng, Q. (2015). A gene-expression-based neural code for food abundance that modulates lifespan. *eLife* 4, e06259.
- Fielenbach, N., and Antebi, A. (2008). *C. elegans* dauer formation and the molecular basis of plasticity. *Genes Dev.* 22, 2149–2165.
- Flavell, S.W., Pokala, N., Macosko, E.Z., Albrecht, D.R., Larsch, J., and Bargmann, C.I. (2013). Serotonin and the neuropeptide PDF initiate and extend opposing behavioral states in *C. elegans*. *Cell* 154, 1023–1035.

- Freedman, D., and Diaconis, P. (1981). On the histogram as a density estimator: L_2 theory. *Probab. Theory Relat. Fields* 57, 453–476.
- Fujiwara, M., Sengupta, P., and McIntire, S.L. (2002). Regulation of body size and behavioral state of *C. elegans* by sensory perception and the EGL-4 cGMP-dependent protein kinase. *Neuron* 36, 1091–1102.
- Greene, J.S., Brown, M., Dobosiewicz, M., Ishida, I.G., Macosko, E.Z., Zhang, X., Butcher, R.A., Cline, D.J., McGrath, P.T., and Bargmann, C.I. (2016). Balancing selection shapes density-dependent foraging behaviour. *Nature* 539, 254–258.
- Grosse, I., Bernaola-Galván, P., Carpena, P., Román-Roldán, R., Oliver, J., and Stanley, H.E. (2002). Analysis of symbolic sequences using the Jensen-Shannon divergence. *Phys. Rev. E. Stat. Nonlin. Soft Matter Phys.* 65, 041905.
- Gürel, G., Gustafson, M.A., Pepper, J.S., Horvitz, H.R., and Koelle, M.R. (2012). Receptors and other signaling proteins required for serotonin control of locomotion in *Caenorhabditis elegans*. *Genetics* 192, 1359–1371.
- Hamdan, F.F., Ungrin, M.D., Abramovitz, M., and Ribeiro, P. (1999). Characterization of a novel serotonin receptor from *Caenorhabditis elegans*: cloning and expression of two splice variants. *J. Neurochem.* 72, 1372–1383.
- Hendriks, G.-J., Gaidatzis, D., Aeschmann, F., and Großhans, H. (2014). Extensive oscillatory gene expression during *C. elegans* larval development. *Mol. Cell* 53, 380–392.
- Hobson, R.J., Geng, J., Gray, A.D., and Komuniecki, R.W. (2003). SER-7b, a constitutively active Galphas coupled 5-HT7-like receptor expressed in the *Caenorhabditis elegans* M4 pharyngeal motoneuron. *J. Neurochem.* 87, 22–29.
- Jane Garland, E., Kutcher, S., Virani, A., and Elbe, D. (2016). Update on the use of SSRIs and SNRIs with children and adolescents in clinical practice. *J. Can. Acad. Child Adolesc. Psychiatry* 25, 4–10.
- Jin, X., Pokala, N., and Bargmann, C.I. (2016). Distinct circuits for the formation and retrieval of an imprinted olfactory memory. *Cell* 164, 632–643.
- Jordan, D., Kuehn, S., Katifori, E., and Leibler, S. (2013). Behavioral diversity in microbes and low-dimensional phenotypic spaces. *Proc. Natl. Acad. Sci. USA* 110, 14018–14023.
- Kain, J.S., Stokes, C., and de Bivort, B.L. (2012). Phototactic personality in fruit flies and its suppression by serotonin and white. *Proc. Natl. Acad. Sci. USA* 109, 19834–19839.
- Kimmel, C.B., Patterson, J., and Kimmel, R.O. (1974). The development and behavioral characteristics of the startle response in the zebra fish. *Dev. Psychobiol.* 7, 47–60.
- Konopka, R.J., and Benzer, S. (1971). Clock mutants of *Drosophila melanogaster*. *Proc. Natl. Acad. Sci. USA* 68, 2112–2116.
- Lin, J. (1991). Divergence measures based on the Shannon entropy. *IEEE Trans. Inf. Theory* 37, 145–151.
- Lorenz, K. (1935). Der Kumpan in der Umwelt des Vogels. *J. Ornithol.* 83, 137–213, 289–413.
- Mello, C.C., and Conte, D., Jr. (2004). Revealing the world of RNA interference. *Nature* 431, 338–342.
- Nottebohm, F. (1968). Auditory experience and song development in the chaffinch *fringilla coelebs*. *Ibis* 110, 549–568.
- Olde, B., and McCombie, W.R. (1997). Molecular cloning and functional expression of a serotonin receptor from *Caenorhabditis elegans*. *J. Mol. Neurosci.* 8, 53–62.
- Omura, D.T., Clark, D.A., Samuel, A.D.T., and Horvitz, H.R. (2012). Dopamine signaling is essential for precise rates of locomotion by *C. elegans*. *PLoS ONE* 7, e38649.
- Park, J.H., and Hall, J.C. (1998). Isolation and chronobiological analysis of a neuropeptide pigment-dispersing factor gene in *Drosophila melanogaster*. *J. Biol. Rhythms* 13, 219–228.
- Pattwell, S.S., Duhoux, S., Hartley, C.A., Johnson, D.C., Jing, D., Elliott, M.D., Ruberry, E.J., Powers, A., Mehta, N., Yang, R.R., et al. (2012). Altered fear learning across development in both mouse and human. *Proc. Natl. Acad. Sci. USA* 109, 16318–16323.
- Pincus, Z., Smith-Vikos, T., and Slack, F.J. (2011). MicroRNA predictors of longevity in *Caenorhabditis elegans*. *PLoS Genet.* 7, e1002306.
- Raizen, D.M., Zimmerman, J.E., Maycock, M.H., Ta, U.D., You, Y.J., Sundaram, M.V., and Pack, A.I. (2008). Lethargus is a *Caenorhabditis elegans* sleep-like state. *Nature* 451, 569–572.
- Raj, A., Rifkin, S.A., Andersen, E., and van Oudenaarden, A. (2010). Variability in gene expression underlies incomplete penetrance. *Nature* 463, 913–918.
- Rakyan, V.K., Blewitt, M.E., Druker, R., Preis, J.I., and Whitelaw, E. (2002). Metastable epialleles in mammals. *Trends Genet.* 18, 348–351.
- Ranganathan, R., Cannon, S.C., and Horvitz, H.R. (2000). MOD-1 is a serotonin-gated chloride channel that modulates locomotory behaviour in *C. elegans*. *Nature* 408, 470–475.
- Rea, S.L., Wu, D., Cypser, J.R., Vaupel, J.W., and Johnson, T.E. (2005). A stress-sensitive reporter predicts longevity in isogenic populations of *Caenorhabditis elegans*. *Nat. Genet.* 37, 894–898.
- Rehm, K.J., Deeg, K.E., and Marder, E. (2008). Developmental regulation of neuromodulator function in the stomatogastric ganglion of the lobster, *Homarus americanus*. *J. Neurosci.* 28, 9828–9839.
- Riddle, D.L., Swanson, M.M., and Albert, P.S. (1981). Interacting genes in nematode dauer larva formation. *Nature* 290, 668–671.
- Sandler, O., Mizrahi, S.P., Weiss, N., Agam, O., Simon, I., and Balaban, N.Q. (2015). Lineage correlations of single cell division time as a probe of cell-cycle dynamics. *Nature* 519, 468–471.
- Saudou, F., Amara, D.A., Dierich, A., LeMeur, M., Ramboz, S., Segu, L., Buhot, M.C., and Hen, R. (1994). Enhanced aggressive behavior in mice lacking 5-HT1B receptor. *Science* 265, 1875–1878.
- Sawin, E.R., Ranganathan, R., and Horvitz, H.R. (2000). *C. elegans* locomotory rate is modulated by the environment through a dopaminergic pathway and by experience through a serotonergic pathway. *Neuron* 26, 619–631.
- Schuett, W., Dall, S.R.X., Baeumer, J., Kloesener, M.H., Nakagawa, S., Beinlich, F., and Eggers, T. (2011). Personality variation in a clonal insect: the pea aphid, *Acyrtosiphon pisum*. *Dev. Psychobiol.* 53, 631–640.
- Schwarz, R.F., Branicky, R., Grundy, L.J., Schafer, W.R., and Brown, A.E.X. (2015). Changes in postural syntax characterize sensory modulation and natural variation of *C. elegans* locomotion. *PLoS Comput. Biol.* 11, e1004322.
- Shannonhouse, J.L., DuBois, D.W., Fincher, A.S., Vela, A.M., Henry, M.M., Wellman, P.J., Frye, G.D., and Morgan, C. (2016). Fluoxetine disrupts motivation and GABAergic signaling in adolescent female hamsters. *Prog. Neuropsychopharmacol. Biol. Psychiatry* 69, 19–30.
- Shtonda, B.B., and Avery, L. (2006). Dietary choice behavior in *Caenorhabditis elegans*. *J. Exp. Biol.* 209, 89–102.
- Sisk, C.L., and Foster, D.L. (2004). The neural basis of puberty and adolescence. *Nat. Neurosci.* 7, 1040–1047.
- Slatkin, M. (1974). Hedging one's evolutionary bets. *Nature* 250, 704–705.
- Sokolowski, M.B. (1980). Foraging strategies of *Drosophila melanogaster*: a chromosomal analysis. *Behav. Genet.* 10, 291–302.
- Sokolowski, M.B., Kent, C., and Wong, J. (1984). *Drosophila* larval foraging behaviour: Developmental stages. *Anim. Behav.* 32, 645–651.
- Song, B.M., Faumont, S., Lockery, S., and Avery, L. (2013). Recognition of familiar food activates feeding via an endocrine serotonin signal in *Caenorhabditis elegans*. *eLife* 2.
- Spencer, S.L., Gaudet, S., Albeck, J.G., Burke, J.M., and Sorger, P.K. (2009). Non-genetic origins of cell-to-cell variability in TRAIL-induced apoptosis. *Nature* 459, 428–432.
- Süel, G.M., Garcia-Ojalvo, J., Liberman, L.M., and Elowitz, M.B. (2006). An excitable gene regulatory circuit induces transient cellular differentiation. *Nature* 440, 545–550.
- Sulston, J., Dew, M., and Brenner, S. (1975). Dopaminergic neurons in the nematode *Caenorhabditis elegans*. *J. Comp. Neurol.* 163, 215–226.

- Sze, J.Y., Victor, M., Loer, C., Shi, Y., and Ruvkun, G. (2000). Food and metabolic signalling defects in a *Caenorhabditis elegans* serotonin-synthesis mutant. *Nature* 403, 560–564.
- Troemel, E.R., Sagasti, A., and Bargmann, C.I. (1999). Lateral signaling mediated by axon contact and calcium entry regulates asymmetric odorant receptor expression in *C. elegans*. *Cell* 99, 387–398.
- Truman, J.W. (2005). Hormonal control of insect ecdysis: endocrine cascades for coordinating behavior with physiology. *Vitam. Horm.* 73, 1–30.
- Wadsworth, W.G., and Riddle, D.L. (1989). Developmental regulation of energy metabolism in *Caenorhabditis elegans*. *Dev. Biol.* 132, 167–173.
- Weksberg, R., Shuman, C., Caluseriu, O., Smith, A.C., Fei, Y.-L., Nishikawa, J., Stockley, T.L., Best, L., Chitayat, D., Olney, A., et al. (2002). Discordant KCNQ1OT1 imprinting in sets of monozygotic twins discordant for Beckwith-Wiedemann syndrome. *Hum. Mol. Genet.* 11, 1317–1325.
- Wenzel, D., Palladino, F., and Jedrusik-Bode, M. (2011). Epigenetics in *C. elegans*: facts and challenges. *Genesis* 49, 647–661.
- Wigglesworth, V.B. (1936). Memoirs: The function of the corpus allatum in the growth and reproduction of *Rhodnius prolixus* (Hemiptera). *J. Cell Sci.* s2-79, 91–121.
- Wiltschko, A.B., Johnson, M.J., Iurilli, G., Peterson, R.E., Katon, J.M., Pashkovski, S.L., Abaira, V.E., Adams, R.P., and Datta, S.R. (2015). Mapping sub-second structure in mouse behavior. *Neuron* 88, 1121–1135.
- Witz, P., Amlaiky, N., Plassat, J.L., Maroteaux, L., Borrelli, E., and Hen, R. (1990). Cloning and characterization of a *Drosophila* serotonin receptor that activates adenylate cyclase. *Proc. Natl. Acad. Sci. USA* 87, 8940–8944.
- Wong, A.H.C., Gottesman, I.I., and Petronis, A. (2005). Phenotypic differences in genetically identical organisms: the epigenetic perspective. *Hum. Mol. Genet.* 14, R11–R18.
- Yeh, S.R., Fricke, R.A., and Edwards, D.H. (1996). The effect of social experience on serotonergic modulation of the escape circuit of crayfish. *Science* 271, 366–369.

STAR★METHODS

KEY RESOURCES TABLE

REAGENT or RESOURCE	SOURCE	IDENTIFIER
Deposited Data		
Behavior dataset	This study	https://data.mendeley.com/datasets/3j6fsr634d/draft?a=9ae11db1-7149-486e-8591-9209817f39aa
Experimental Models: Organisms/Strains		
Wild-type Bristol N2	N/A	N/A
<i>tph-1(mg280) II</i>	H.R. Horvitz lab, MIT	MT15434
<i>cat-2(e1112) II</i>	Bargmann lab	CX11078
<i>tdc-1(n3420) II</i>	H.R. Horvitz lab, MIT	MT10548
<i>npr-1(ad609) X</i>	Bargmann lab	CX13663
<i>daf-7(e1372) III</i>	H.R Horvitz lab, MIT	CB1372
<i>ser-1(ok345) X</i>	L. Avery lab, UTSW	DA1814
<i>ser-4(ok512) III</i>	CGC	AQ866
<i>ser-5(tm2647) I</i>	Bargmann lab	CX13075
<i>ser-7(tm1325) X</i>	L. Avery lab, UTSW	DA2100
<i>mod-1(ok103) V</i>	CGC	MT9668
<i>mod-5(n822) I</i>	Bargmann lab	CX13630
Software and Algorithms		
FlyCapture	Pointgrey	https://www.ptgrey.com/
MATLAB (version 2014b)	Mathworks	https://www.mathworks.com
Analysis scripts (Python, MATLAB)	This study	https://github.com/ChristophKirst/CelegansLongTermBehavioralAnalysis
Other		
8.8 MP USB3 Flea camera	Pointgrey	Cat#FL3-U3-88S2C-C
LED backlights	Metaphase Technologies	Cat#99021169
Temperature control (cooling unit- Peltier element)	TE technology	Cat#AC-027

CONTACT FOR REAGENT AND RESOURCE SHARING

Further information and requests for resources and reagents should be directed to and will be fulfilled by Lead Contact, Cornelia I. Bargmann (cori@rockefeller.edu).

EXPERIMENTAL MODEL AND SUBJECT DETAILS

C. elegans strains

Strains used in this study are:

Wild-type Bristol N2
 MT15434 *tph-1(mg280) II* (backcrossed at MIT)
 CX11078 *cat-2(e1112) II* (backcrossed 6X)
 MT10548 *tdc-1(n3420) II* (backcrossed at MIT)
 CX13663 *npr-1(ad609) X* (backcrossed 4X)
 CB1372 *daf-7(e1372) III*
 DA1814 *ser-1(ok345) X* (backcrossed 10X)
 AQ866 *ser-4(ok512) III* (backcrossed 5X)
 CX13075 *ser-5(tm2647) I* (backcrossed 5X)

DA2100 *ser-7(tm1325) X* (backcrossed 10X)
MT9668 *mod-1(ok103) V* (backcrossed 6X)
CX13630 *mod-5(n822) I* (backcrossed 3X)

Growth conditions

Populations were maintained on NGM agar plates supplemented with *E. coli* OP50 bacteria. For behavioral imaging, isogenic populations of worms were bleached to isolate eggs, and single eggs were transferred (using 2 μ L of M9 buffer) to a custom-made laser-cut multi-well plate. Each individual was placed in its own circular arena of diameter 10 mm, height 1.5 mm, containing NGM agar supplemented with a defined amount of concentrated OP50 bacteria (10 μ L of 1.5 OD stock, UV killed immediately after seeding the plates to prevent bacterial growth during the experiment). Control experiments with N2 demonstrated that bleaching eggs did not affect the behavior of the offspring.

METHOD DETAILS

Imaging system

The imaging system consists of an array of six 8.8 MP USB3 cameras (Pointgrey, Flea3) and 35 mm high-resolution objectives (Edmund optics) mounted on optical construction rails (Thorlabs). Each camera images up to six individuals grown in isolation, capturing movies at 3 fps with a spatial resolution of \sim 10 μ m. For uniform illumination of the imaging plates we used identical LED backlights (Metaphase Technologies) and polarization sheets. To tightly control environmental parameters during the experiment, imaging was conducted inside a custom-made environmental chamber in which temperature was controlled using a Peltier element (TE technologies, temperature fluctuations in the range of $22 \pm 0.07^\circ\text{C}$), humidity was held in the range of 50% \pm 5% with a sterile water reservoir, and outside illumination was blocked, keeping the internal LED backlights as the only illumination source. Movies from the cameras were captured using commercial software (FlyCapture, Pointgrey) and saved on two computers (3 cameras per computer; each computer has a 4 core Intel i7 processor and 64 GB RAM).

Behavioral trajectory extraction from imaging data

To extract behavioral trajectories of animals along the time-course of the experiment, captured movies were analyzed by custom-made script programmed in MATLAB (Mathworks, version 2014b) using the image processing toolbox. In each frame of the movie and for each behavioral arena, the worm is automatically detected as a moving object by background subtraction, and its XY position is logged (center of mass). In each experiment 15-20 million frames are analyzed using 96 computer processors in parallel, distributed between 4 computers (each computer has a 24 core Intel Xeon processor, and 128 GB of RAM), to reconstruct the full behavioral trajectory of individuals over days of measurements. The total time of image processing was 2.5 days per experiment. Egg hatching time of every individual in the experiment is automatically marked by the time when activity can be detected in the behavioral arena. To detect time periods along the experiment that correspond to the different post-embryonic *C. elegans* life-stages (L1-L4 larval stages and the adult stage) we marked the middle of the lethargus periods, in which animals stop their locomotion and molt, as the transition points between different life stages (based on speed trajectories over time, smoothed over 300 frames). To synchronize behavioral trajectories of different individuals in time within and across genotypes, we age-normalized individuals by dividing the behavioral trajectory of each life stage into a fixed number of time bins. Long-term behavioral structures were tightly correlated to the animal's development, and not correlated to the time of day in the experiment.

Heritability experiments

The behavior of an N2 wild-type parental population was recorded from egg hatching to adulthood for 55 hours, then individuals were separately transferred to agar plates seeded with OP50 bacteria to generate F1 progeny. In parallel, the parental movies were analyzed using 96 computer processors to identify two individuals from the parental population that showed extreme individuality (consistent roamer and consistent dweller), a process that took 2.5 days overlapping the development of the F1 progeny. 70-100 adult F1 progeny of the two persistent individuals were picked and F2 eggs were isolated for analysis from both populations. The behavior of F2 animals that hatched from these eggs was recorded for 55 hours under standard conditions.

QUANTIFICATION AND STATISTICAL ANALYSES

Quantification of behavioral parameters

We classified roaming and dwelling states in each individual by averaging speed ($\mu\text{m/s}$) and angular velocity (absolute deg/s) over 10 s using a rolling time window, and generating a 2D probability distribution of these two behavioral parameters for all intervals in each time-bin along the experiment (50 X 50 bins distribution, speed bin size: 6 $\mu\text{m/s}$, angular velocity bin size: 3.6 deg/s). Drawing a diagonal through the probability distribution separated roaming and dwelling intervals, such that intervals in the distribution bins below the diagonal were classified as roaming intervals and intervals in bins above the diagonal were classified as dwelling intervals (Ben Arous et al., 2009; Flavell et al., 2013). The behavior of each animal could then be described as a sequence of roaming and

dwelling intervals. The fraction of these intervals classified as roaming states within a given time bin represented the fraction of time roaming of the individual in that time bin. For each life stage, we examined the two-dimensional probability distribution of the whole population and changed the slope of the diagonal to classify roaming and dwelling appropriately (Figure S1, slopes: 5,2.5,2.3,2,1.5 for the L1,L2,L3,L4 and adult stages, respectively). Based on these roaming and dwelling classifications we then quantified two additional behavioral parameters in each time bin: the average instantaneous speed of the animal during roaming episodes ($\mu\text{m/s}$), and speed variability during roaming episodes (coefficient of variation, CV).

Quantification of behavioral individuality

Individuals within the population were ranked based on their behavior in 50 time bins (10 per stage), from the individual with the highest value to the individual with the lowest value. We then quantified the consistent bias in the individual's behavior relative to the population by calculating for each individual the $\log_2(\text{number of time bins in which the individual's rank is higher than the population median} / \text{number of time bins in which the individual's rank is lower than the population median})$ ('consistency index'). This measure gives positive values to individuals that tend to have higher than median ranks across time, negative values to individuals that tend to have lower than median ranks across time, and values close to 0 for individuals that do not show any bias toward higher or lower ranks. The statistical significance of consistency in each individual (Figures 2, S5, and S6) was calculated by bootstrapping, comparing the individual's consistency index to consistency indices of 1000 randomly generated individuals from a shuffled dataset of the same population (p values of individuals were corrected for multiple hypotheses testing using FDR). In a parallel analysis, very similar consistencies were captured by using the Fisher-Pearson coefficient of skewness ($R = 0.89\text{-}0.93$ across genotypes), as a measure of the individual's rank distribution bias. No technical biases were observed across experiments done on different days or across different positions in the experimental setup.

Comparisons between consistency in mutant versus N2 populations (Figures 4 and 6) was performed by comparing the fractions of individuals that showed significant consistency in the mutant strain with a randomly picked wild-type subpopulation of the same size as the mutant population. This procedure was repeated 1000 times to generate a statistical significance value for each mutant strain that was corrected for multiple hypothesis testing using FDR. We also verified significance of differences between strains using a Chi-square statistical test.

Quantification of differences in behavior between genotypes

To quantify behavioral differences between mutants and wild-type populations in roaming fraction, roaming speed, and roaming speed variability (Figures 4, 6, S4, and S6) we estimated the probability density of each of these behavioral parameters over time for each population via histograms. Histogram bin widths and numbers were estimated via the Freedman-Diaconis rule (Freedman and Diaconis, 1981). Differences of the distribution p at a specified time bin to the wild-type distribution q was then quantified via the symmetric and bounded Jensen-Shannon divergence (Lin, 1991)

$$D_{JS}(p, q) = \frac{1}{2}(D_{KL}(p | m) + D_{KL}(q | m))$$

where D_{KL} is the Kullback-Leibler divergence and $m = (1/2)(p + q)$ the average distribution. To highlight an overall increase or decrease in the parameters we multiplied D_{JS} by the sign of the difference in the means of the behavioral parameters in each time bin. Statistical significance for the Jensen-Shannon divergences was estimated analytically (Grosse et al., 2002)

$$P(D_{JS} \leq x) \approx \frac{\Gamma(\nu/2, xN \ln(2))}{\Gamma(\nu/2)}$$

where N is the number of samples, $\nu = \#bins - 1$, Γ is the (in)complete gamma function. P values were corrected for multiple hypothesis testing using FDR. Significance results were confirmed via bootstrapping.

DATA AND SOFTWARE AVAILABILITY

The data accompanying this paper have been deposited into Mendeley (<https://data.mendeley.com/datasets/3j6fsr634d/draft?a=9ae11db1-7149-486e-8591-9209817f39aa>). Analysis scripts have been deposited into GitHub (<https://github.com/ChristophKirst/CelegansLongTermBehavioralAnalysis>).

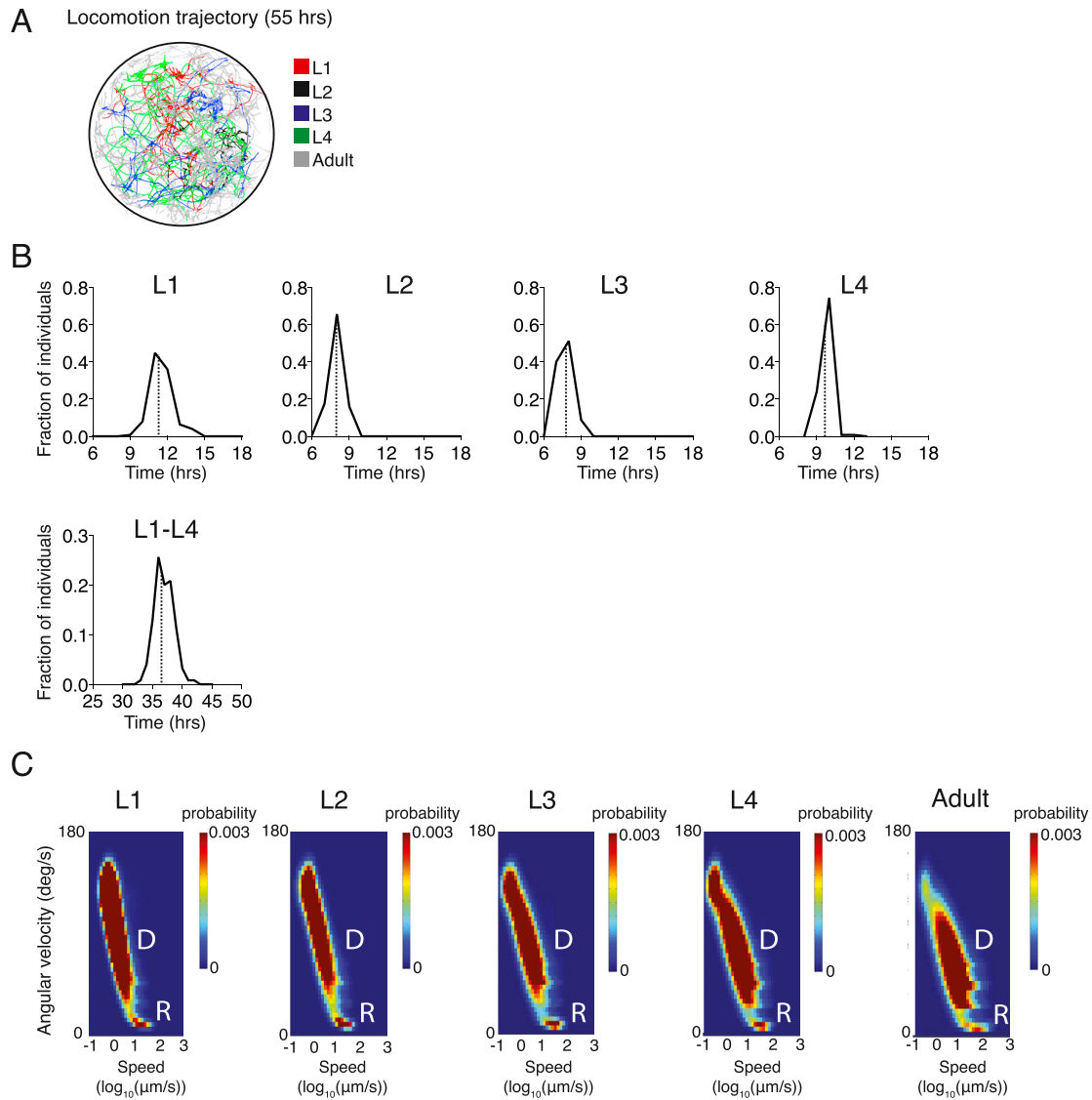


Figure S1. Development Time and Roaming and Dwelling Classification in Wild-Type Individuals, Related to Figure 1 and STAR Methods
 (A) Locomotion trajectory of a single individual across 55 hours encompassing hatching to the adult stage.
 (B) Variation among wild-type individuals in the duration of each larval stage (upper panels), and measured from egg hatching to start of adulthood (bottom panel) ($n = 125$ individuals). Average development time is indicated by the dashed line.
 (C) Two-dimensional probability distributions of speed ($\mu\text{m/s}$) and angular velocity (degrees/s) averaged over 10 s time windows for 125 wild-type N2 individuals, demonstrating distinguishable roaming (R) and dwelling (D) states in each developmental stage.

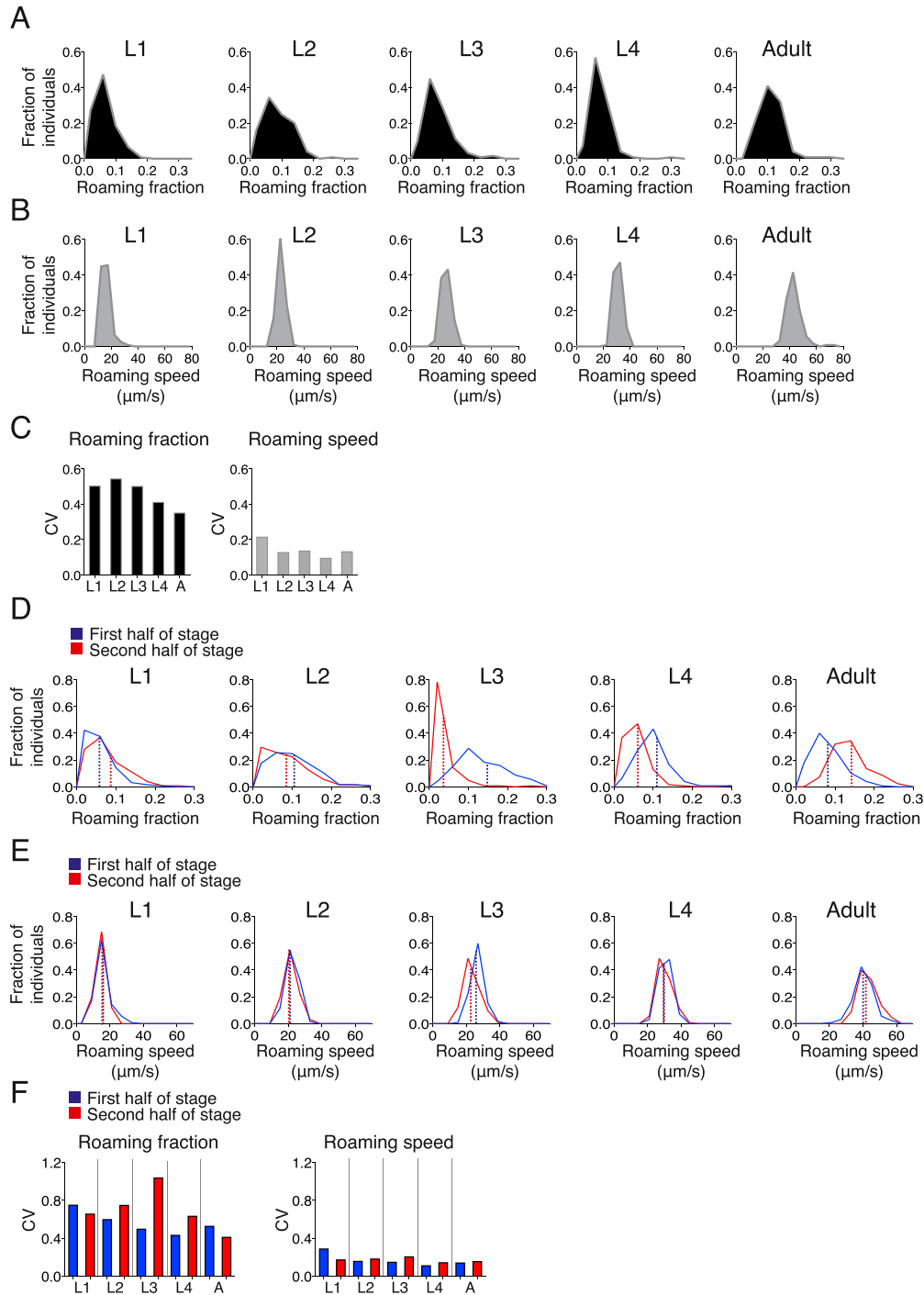


Figure S2. Roaming Fraction and Roaming Speed Distributions of Wild-Type Individuals, Related to Figure 1

(A) Distributions of the average fraction of time roaming in wild-type individuals across stages ($n = 125$).

(B) Distributions of average roaming speed of wild-type individuals across stages.

(C) Coefficient of variation (CV) of roaming fraction (left) and roaming speed (right) distributions across stages.

(D) Distributions of the average fraction of time roaming of individuals in the first half (blue) and second half (red) of the stage. Mean indicated by dashed lines.

(E) Distributions of the average roaming speed of individuals in the first half (blue) and second half (red) of the stage. Mean indicated by dashed lines.

(F) Coefficients of variation (CV) of roaming fraction (left) and roaming speed (right) distributions of the first half (blue) and second half (red) of the stage (data from D and E).

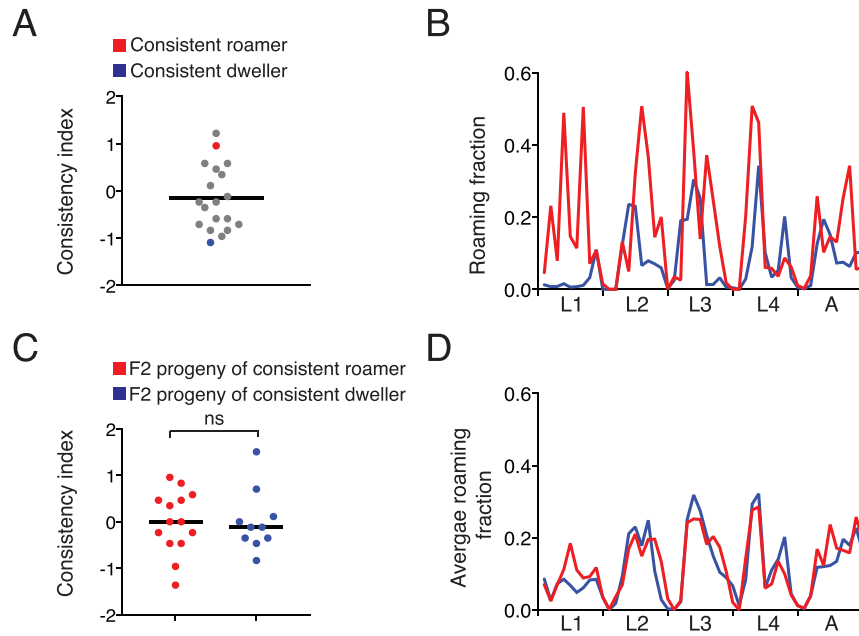


Figure S3. Individuality in Roaming and Dwelling Behavior Is Not Heritable, Related to Figure 2

(A) Roaming fraction consistency in 19 wild-type animals monitored in a single experiment. An individual that consistently roamed more (red) and an individual that consistently roamed less (blue) were selected to generate F2 populations.

(B) Roaming fraction across time of individuals marked in red and blue in (A).

(C) Roaming fraction consistency in randomly selected F2 progeny of the red and blue animals from A; $n = 14$ and 10 , respectively. The consistency index was calculated relative to the combined F2 population shown here. Statistical significance was calculated using Wilcoxon rank test.

(D) Average roaming fraction across time for animals shown in (C).

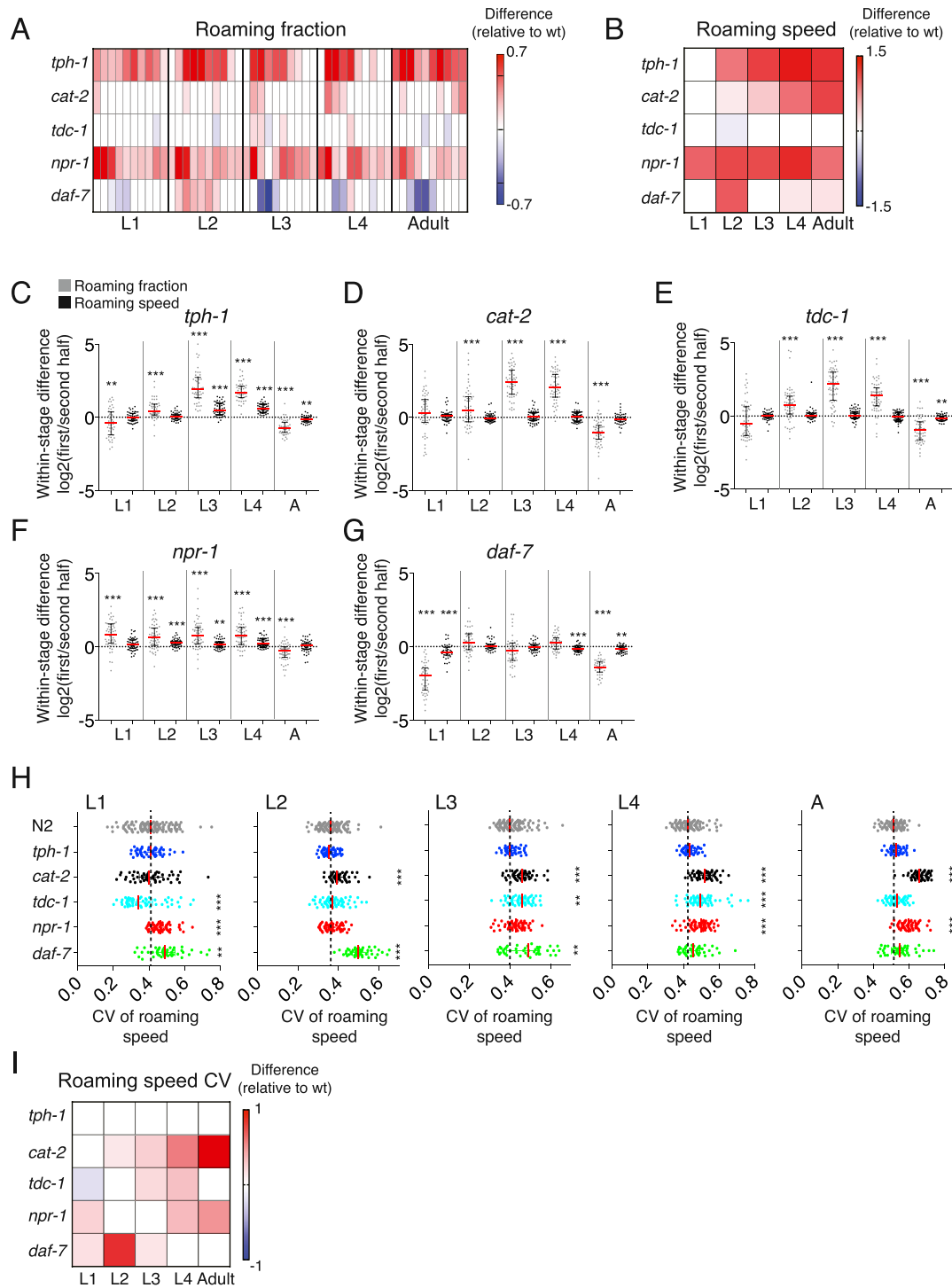


Figure S4. Roaming Fraction, Roaming Speed, and Speed Variability of Neuromodulatory Mutants, Related to Figures 3 and 4

(A) Summary of roaming fraction differences between mutants and wild-type population distributions across all developmental stages (10 time bins per stage). Color represents positive (red, higher roaming in mutant) or negative (blue, lower roaming in mutant) differences (JS divergence). Non-significant distances ($p > 0.01$, JS divergence, FDR corrected) are in white.

(B) Summary of roaming speed differences between mutants and wild-type populations across all developmental stages (1 bin per stage). Color represents positive (higher speed in mutant) or negative (lower speed in mutant) differences (JS divergence). Non-significant distances ($p > 0.01$ JS divergence, FDR corrected) are in white.

(legend continued on next page)

(C–G) Comparison of roaming fraction and roaming speed between the first and second half of each stage (L1 to adult) in mutant individuals, calculated for each individual as $\log_2(\text{behavior in 1}^{\text{st}} \text{ half}/\text{behavior in 2}^{\text{nd}} \text{ half})$. Asterisks represent the significance of difference between the first and second half of each stage. ** $p < 0.01$, *** $p < 0.001$ (Wilcoxon rank test). Red bars represent population mean, and black bars represent Q1–Q3 range.

(H) Roaming speed variability (coefficient of variation, CV) of mutant individuals compared to wild-type individuals across developmental stages. Dashed line indicated the median of the N2 population in each stage. ** $p < 0.01$, *** $p < 0.001$ (JS divergence, FDR corrected).

(I) Summary of differences in roaming speed variability between mutants and wild-type populations across all developmental stages (1 bin per stage). Color represents positive (higher value in mutant) or negative (lower value in mutant) distances (JS divergence). Non-significant distances ($p > 0.01$, JS divergence, FDR corrected) are marked in white.

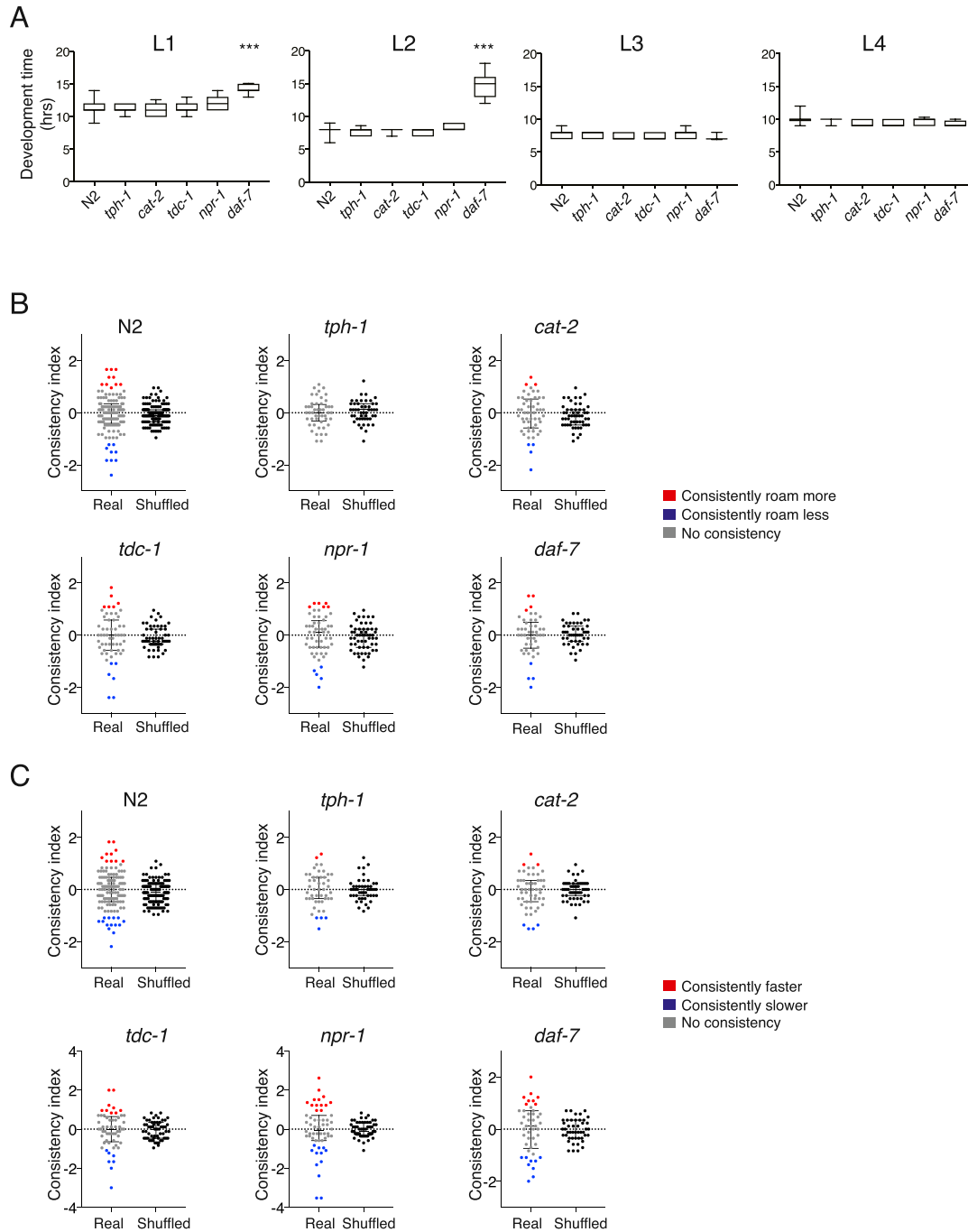


Figure S5. Development Time and Behavioral Consistency of Neuromodulatory Mutants, Related to Figures 3 and 4

(A) Duration of L1, L2, L3, and L4 larval stage in neuromodulatory mutants and wild-type animals. Distributions are represented by boxplots (whiskers shows 5-95 percentile range). Only *daf-7* mutations lead to altered developmental timing, consistent with their role in the decision to form a dauer larva, which is made at the end of the L1 stage and expressed during the L2 stage (L2d) and at the end of the L2 stage (dauer formation). Individuals shown here did not become dauer larvae. *** $p < 0.001$ (Wilcoxon test, FDR corrected) and average difference > 1 hour, relative to wild-type.

(B) Roaming fraction consistency in mutant individuals that show significant positive roaming consistency (consistently roam more, red), significant negative roaming consistency (consistently roam less, blue), or no consistency (gray), compared to shuffled dataset of the same number of individuals (black). Black bars represent Q1-Q3 range.

(C) Roaming speed consistency in mutant individuals that show significant positive roaming speed consistency (consistently faster, red), significant negative roaming speed consistency (consistently slower, blue), or no consistency (gray), compared to shuffled dataset of the same number of individuals (black). Statistical significance was calculated for each individual by bootstrapping (False Discovery Rate (adjusted p value) < 0.05). Black bars represent Q1-Q3 range.

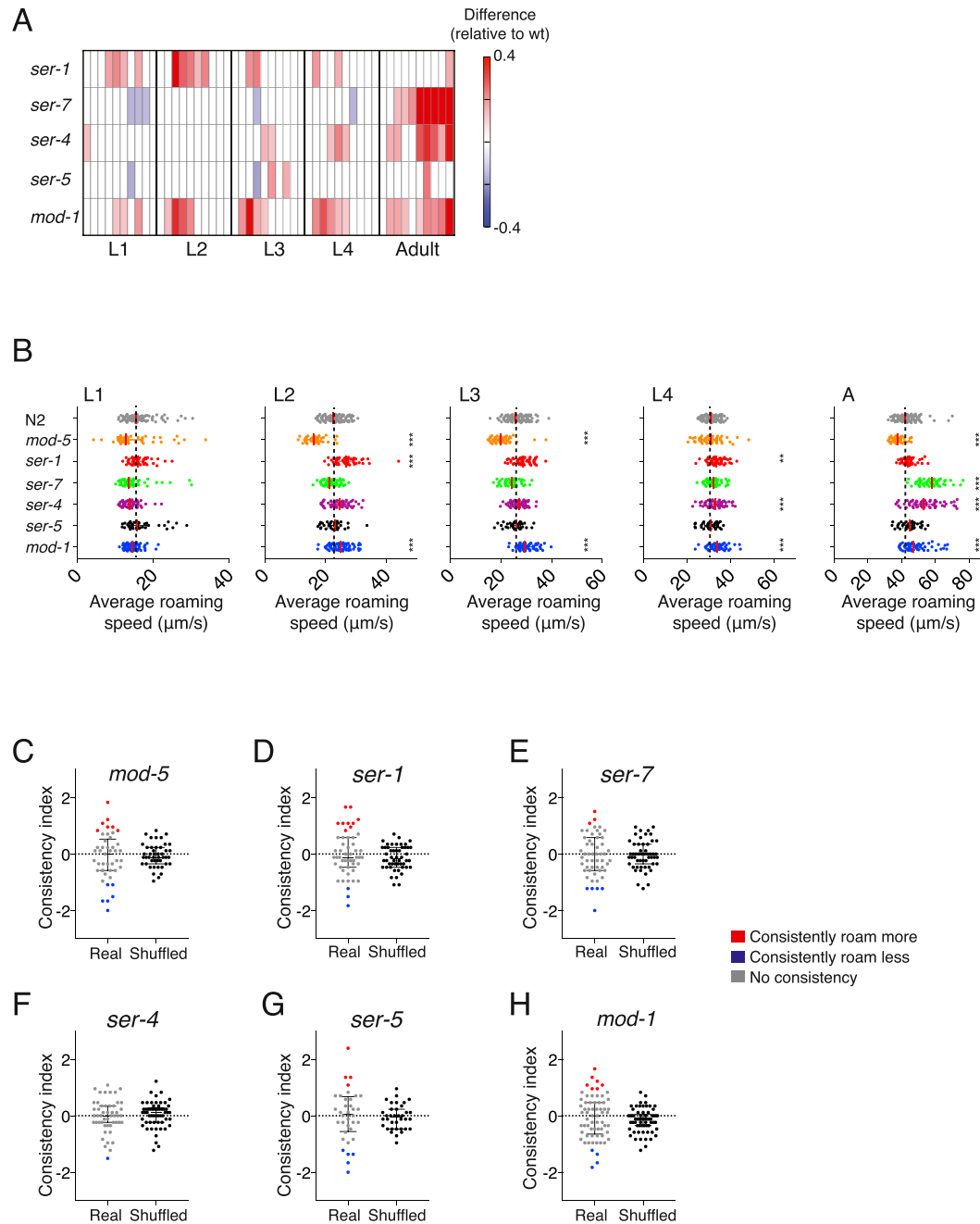


Figure S6. Roaming Fraction, Roaming Speed, and Behavioral Consistency of Serotonin Receptor Mutants, Related to Figures 5 and 6

(A) Summary of roaming fraction differences between serotonin receptor mutants and wild-type population distributions across all developmental stages (10 time bins per stage). Color represents positive (red, higher roaming in mutant) or negative (blue, lower roaming in mutant) differences (JS divergence). Non-significant distances ($p > 0.01$, JS divergence, FDR corrected) are in white.

(B) Average roaming speed of serotonin receptor and serotonin reuptake transporter mutant individuals compared to wild-type individuals across developmental stages. Each point represents an animal, red bars represent population mean, dashed line indicates the average of the N2 population in each stage. ** $p < 0.01$, *** $p < 0.001$ (JS divergence, FDR corrected).

(C–H) Roaming fraction consistency in serotonin receptor and serotonin reuptake channel mutant individuals, with significant positive roaming consistency (consistently roam more, red), significant negative roaming consistency (consistently roam less, blue), or no consistency (gray), compared to shuffled dataset of the same number of individuals (black). Statistical significance was calculated for each individual by bootstrapping (False Discovery Rate (adjusted p value) < 0.05). Black bars represent Q1–Q3 range.